ESTIMATION OF MEMBER FORCES IN FATIH SULTAN MEHMET (FSM) SUSPENSION BRIDGE FROM AMBIENT VIBRATION RECORDS

by

Yavuz Kavak

B.S., Civil Engineering, Kocaeli University, 2013

B.S., Geophysical Engineering, Kocaeli University, 2012

Submitted to the Kandilli Observatory and Earthquake Research Institute
in partial fulfillment of the requirements for the degree of
Master of Science

Graduate Program in Earthquake Engineering

Boğaziçi University

2019

ACKNOWLEDGEMENTS

I would like to express my deepest appreciation to my advisor Prof. Dr. Erdal Şafak for the continuous support of my study, for his patience, motivation, enthusiasm, immense knowledge and my time at KOERI. His guidance helped me in all the time of research and writing of this thesis. Thank you for providing me with this opportunity, and I really appreciate that.

I would like to express my special thanks to all my lecturers in Bogaziçi University, Department of Earthquake Engineering and Kocaeli University, Department of Civil Engineering and Geophysical Engineering for their precious assistance, theoretical and practical knowledge and passion.

On the other hand I would like to express my sincere thanks to my dear colleagues Mahir Çetin and Hakan Doğukan Savaş for their assistance during my thesis.

Special thanks go to the staff at Karayolları Genel Müdürlüğü and the Fatih Sultan Mehmet suspension bridge for giving us access to their bridge for my research.

Finally, many thanks to Mr Ahmet Korkmaz and Mr Mehmet Nafiz Kafadar for their guidance and assistance at the site in my data collection.

ABSTRACT

ESTIMATION OF MEMBER FORCES IN FATIH SULTAN MEHMET (FSM) SUSPENSION BRIDGE FROM AMBIENT VIBRATION RECORDS

Suspension bridges are critical lifeline structures in transportation systems. Most suspension bridges, built in recent years, have monitoring systems to identify and track any changes in their dynamic characteristics. Such systems are useful for reducing the cost of maintenance during the life of the bridge, as well as assessing the structural safety for any extreme loading condition, such as those induced by large earthquakes and strong winds.

The standard approach for analyzing data from the monitoring systems in suspension bridges has been modal analysis, where the dynamic response is approximated as the sum of modal responses, each defined by its modal frequency, damping ratio and the mode shape, which are identified from vibration records. Theoretically, modal analysis is appropriate for linear structures with mass and/or stiffness proportional viscous damping. Modal analysis is not appropriate for suspension bridges for several reasons. The dynamic behavior of a typical suspension bridge is not linear. Their size and flexibility make them geometrically nonlinear. In addition, their mass is not constant. They have time-varying mass due to moving traffic loads, which can be a significant portion of total mass in modern suspension bridges with lightweight steel decks. Also, all vibration records from suspension bridges show that damping identified, does not satisfy the requirements of classical modal damping (i.e., mass and/or stiffness proportional), and it is not a viscous type. Therefore, alternative methods for the analysis of vibration data from suspension bridges are needed.

This study presents an alternative method for system identification of suspension bridges from their vibration records. Instead of identifying the modal properties of the bridge, the method aims to identify the forces in the principal bridge elements (i.e., main suspension, back-stay and hanger cables and towers). Based on some simplifying

assumptions, this study first develops the equations that relate the element forces to the fundamental frequency of that element. The fundamental frequencies of the elements are identified from the ambient vibration records taken on the element. Using the equations developed, the forces in each element are calculated, and crosscheck to confirm that they satisfy the boundary conditions at element junctions.

The methodology is tested by using the vibration records from one of the suspension bridges in Istanbul. Currently, Istanbul has three suspension bridges over the Bosphorus, and all installed with real-time monitoring systems. These bridges connect Asian and European parts of Istanbul, and are the critical lifelines for the city. The bridge used for the test is the second Bosphorus Bridge, known as the Fatih Sultan Mehmet (FSM) Bridge, which is between the first and the third suspension bridges on the Bosphorus with a daily traffic load of approximately 200,000 vehicles. The bridge is being monitored with a real-time Structural Health Monitoring (SHM) system composed of 44 channels of acceleration sensors.

The forces in the members of the bridge are calculated by the methodology presented in this study. The results are compared to those from previous investigations (e.g., field tests, analytical models and design calculations), and are found to be consistent. The study shows that the fundamental frequencies of members identified from ambient vibration records provide a simple means to estimate the forces in the elements of suspension bridges.

ÖZET

ÇEVRESEL TİTREŞİM KAYDI İLE FATİH SULTAN MEHMET (FSM) ASMA KÖPRÜSÜ ELEMANLARINA AİT KUVVETLERİN TAYİN EDİLMESİ

Asma köprüler, ulaşım sistemlerinde kritik öneme sahip yapılardır. Son yıllarda inşa edilen çoğu asma köprü, dinamik özelliklerinde herhangi bir değişikliği tespit ve takip etmek için izleme sistemlerine sahiptirler. Bu tür sistemler, köprünün ömrü boyunca bakım maliyetini düşürmek, ayrıca büyük depremler ve kuvvetli rüzgarların neden olduğu aşırı yükleme durumlarında yapısal güvenliği değerlendirmek için faydalıdır.

Asma köprülerdeki izleme sistemlerinden gelen verilerin analizi için standart yaklaşım, her bir modal frekans, sönümleme oranı ve mod şekli tarafından tanımlanan dinamik tepkinin modal tepkilerin toplamı olarak titreşim kayıtlarından tanımlanan modal analiz olmuştur. Teorik olarak, modal analiz, kütle ve/veya rijitlik orantılı viskoz sönümleme lineer yapılar için uygundur. Modal analiz birçok nedenden dolayı asma köprüler için uygun değildir. Tipik bir asma köprünün dinamik davranışı lineer değildir. Boyutları ve esnekliği onları geometrik olarak doğrusal olmayan hale getirir. Bununla beraber, kütleleri sabit değildir. Modern asma köprülerdeki toplam kütlenin önemli bir kısmı olabilen hafif çelik tabliye, hareketli trafik yükler nedeniyle zamana bağlı değişen kütleye sahiptir. Ayrıca, asma köprülerdeki tüm kayıtlar, tanımlanan sönümlemenin, klasik modal sönümleme gerekliliklerini (yani, kütle ve/veya rijitlik orantılı) karşılamadığını ve viskoz bir tip olmadığını göstermektedir. Bu nedenle, asma köprülerden titreşim verilerinin analizi için alternatif yöntemlere ihtiyaç vardır.

Bu çalışma, asma köprülerin titreşim kayıtlarından sistem tanımlaması için alternatif bir yöntem sunmaktadır. Köprünün modal özelliklerini belirlemek yerine, bu yöntem ana köprü elemanlarındaki kuvvetleri (yani ana açıklık, kenar açıklık ve askı kabloları ve kuleler) tanımlamayı amaçlar. Bazı basitleştirici varsayımlara dayanarak, bu çalışma öncelikle eleman kuvvetlerini, bu elemanın temel frekansı ile ilişkilendiren denklemleri

geliştirir. Elemanların temel frekansları, elemanlar üzerinde alınan ortam titreşim kayıtlarından tanımlanmaktadır. Geliştirilen denklemleri kullanarak her bir elemandaki kuvvetler hesaplanmaktadır ve eleman birleşim yerlerindeki sınır koşullarını sağladıklarını doğrulamak için çapraz kontrol edilir.

Metodoloji, İstanbul'daki asma köprülerden birinin titreşim kayıtları kullanılarak test edilmiştir. Mevcut durumda İstanbul boğazında üç adet asma köprü bulunmaktadır ve tümünde gerçek zamanlı izleme sistemleri bulunmaktadır. Bu köprüler İstanbul'un Asya ve Avrupa bölgelerini birbirine bağlar ve şehir için kritik öneme sahiptirler. Test için kullanılan köprü, günlük yaklaşık 200,000 araçlık trafik yükü ile Boğaz'ın ilk ve üçüncü asma köprüleri arasında bulunan Fatih Sultan Mehmet (FSM) köprüsü olarak bilinen ikinci Boğaziçi köprüsüdür. Köprü, 44 kanallı ivme sensöründen oluşan gerçek zamanlı Yapısal Sağlığı İzleme sistemi ile izlenmektedir.

Köprü elemanlarındaki kuvvetler bu çalışmada sunulan yöntem ile hesaplanmaktadır. Sonuçlar, önceki araştırmalardan elde edilen sonuçlarla karşılaştırılmıştır (örneğin, saha testleri, analitik modeller ve tasarım hesapları) ve tutarlı olduğu bulunmuştur. Bu çalışma ortam titreşim kayıtlarından tespit edilen elemanların temel frekanslarının, asma köprü elemanlarındaki kuvvetleri tayin etmenin basit bir yolunu sağladığını göstermektedir.

TABLE OF CONTENTS

LIST OF FIGURES

LIST OF TABLES

LIST OF SYMBOLS

α^2	Geometric and elastic effects parameter
Δ	The distance between the hangers
ΔL	The elongation of the back-stay cable
Δs	The corresponding sag at mid-point of the back-stay cable
λ_c	Non-dimensional frequency parameter for cables
λ_d	Non-dimensional frequency parameter for the deck
λ_t	Non-dimensional frequency parameter for towers
A	Cross sectional area of the element
c	Mode number of cable
D	Diameter of the cable
DL	Dead load
d	Midspan sag on the main span cable
E	The modulus of elasticity of the material
f_c	Natural frequency of the c^{th} mode for cables
f_d	Natural frequency of the d^{th} mode for the deck
f_t	Natural frequency of the t^{th} mode for towers
g	The gravitational acceleration
h	Height of the tower
h_b	Buckling length of the tower
H	Axial tension force on the main span cable
H_b	Axial tension force on the back-stay cable
I	Moment of inertia of the element
k	Stiffness of the element
L	The span length
LL	Live load
L_d	Length of the deck in longitudinal direction
L_e	Length of main span cable with sag
L_h	The free hanger length (after the sockets)
L_s	Length of back-stay cable with sag
L^*	Hypotenuse of height of the tower

m	Mass per unit length
N_h	Axial tension force on the hanger cable
P	Axial compression load on the pylon
p	Uniform dead+live load per unit length of the cable
P_b	Buckling load of the pylon
s	Sag at mid-point of the back-stay cable
t	Time
w	Vertical displacement of the component

LIST OF ACRONYMS/ABBREVIATIONS

2D	Two dimensional
3D	Three dimensional
ASCII	American Standard Code for Information Interchange
FAS	Fourier Amplitude Spectra
FEM	Finite Element Model
FFT	Fast Fourier Transform
FSM	Fatih Sultan Mehmet
GPS	Global Positioning System
NMI	National Marine Institute
SFAS	Smoothed Fourier Amplitude Spectra
SHM	Structural Health Monitoring
SNR	Signal to Noise Ratio

1. INTRODUCTION

1.1. General

Over the last two decades structural monitoring applications in civil engineering have increased greatly due to the rapid developments in instrumentation, communication and data storage technologies. New suspension bridges are commonly installed with monitoring systems during and after their construction. Due to their flexibility and the moving traffic loads, the dynamic properties of such ridges can easily be obtained from their ambient vibration records without a need for external excitations, such as strong winds or earthquakes. Data from structural monitoring systems can be a significant part of bridge maintenance. With proper analysis, any defects and deteriorations in the bridge's structural system can be identified from the data.

The standard approach for analyzing data from the monitoring systems in suspension bridges has been the modal analysis, where the dynamic response is approximated as the sum of modal responses, each defined by its modal frequency, damping ratio and the mode shape, which are identified from the vibration records. Theoretically, modal analysis is appropriate for linear structures with mass and/or stiffness proportional viscous damping. Modal analysis is not appropriate for suspension bridges for several reasons. The dynamic behavior of a typical suspension bridge is not linear. Their size and flexibility make them geometrically nonlinear. In addition, their mass is not constant. They have time-varying mass due to moving traffic loads, which can be a significant portion of total mass in modern suspension bridges with lightweight steel decks. Also, all records from suspension bridges show that damping identified does not satisfy the requirements of classical modal damping (i.e., mass and/or stiffness proportional), and it is not a viscous type. Therefore, alternative methods for the analysis of vibration data from suspension bridges are needed.

This study presents an alternative method for system identification of suspension bridges from their vibration records. Instead of identifying the modal properties of the bridge, the method aims to identify the forces in the principal bridge elements (i.e., main suspension, back-stay and hanger cables and towers). Based on some simplifying

assumptions, this study first develops the equations that relate the element forces to the fundamental frequency of that element. The fundamental frequencies of the elements are identified from the ambient vibration records taken on the element. Using the equations developed, the forces in each element are calculated, and crosscheck to confirm that they satisfy the boundary conditions at element junctions.

The methodology is tested by using the vibration records from one of the suspension bridges in Istanbul, the second Bosporus Bridge, also known as the Fatih Sultan Mehmet (FSM) Bridge. The bridge is being monitored in real-time using 44 channels of acceleration sensors.

1.2. Literature Review

During the last two decades, there has been a significant increase in monitoring and system identification of suspension bridges. Several studies have also been done on FSM Bridge. Brownjohn et al. (1992) carried out Finite Element Model (FEM) and ambient vibration test on the FSM Bridge to examine its lateral, vertical and torsional vibration modes. They concluded that the torsional vibration modes and the main span cable modes of the bridge could only be obtained from a 3D FEM. 2D FEM is more appropriate for vertical and lateral modes of vibration. By comparing the results of FEM and ambient vibration survey, they determined that the measured and computed values agreed well at low frequencies, but not at high frequencies. One of the main results of their studies is that, during earthquakes, the effect of asynchronous excitation at pylon bases is crucial and must be taken into account.

Zhi Fang and Jian-qun Wang (2012) introduced a method to evaluate cable forces from their natural frequencies obtained from ambient vibration measurements. A practical formula to evaluate cable forces is recommended based on the transverse vibration equation of a cable and its solution. It is shown that the proposed formula covers both string- or beam-type behaviour and has sufficient accuracy in identifying cable forces.

Abdel-Ghaffar and Stringfellow (1984) studied that a relatively large number of modes are necessary to get a reasonable representation of the response of suspension

bridge analysis. They found that the additional tension force on cable induced by the lateral excitation of the bridge has negligible effect in comparison to the cable tension due to dead loads and therefore cable tension from lateral excitation can be neglected.

Caetano (2011) performed a series of tests to assess the influence of various parameters on cable forces, such as the bending stiffness, sag, level of stress and constraints at the anchorages. It is shown that the combination of a numerical model and high quality data from ambient or forced vibration tests constitute an extremely valuable tool for accurate identification of cable forces.

Apaydın (2002) studied the dynamic response of the FSM Bridge and developed a 3D FEM using beam elements. The study also utilized data from seismometers and Global Positioning System (GPS) units placed on the bridge. Dynamic properties identified from the data are compared with those from the 3D FEM. The results showed good agreement for the lateral and vertical modes, but not for torsional modes. This was due to the fact he beam elements were not appropriate to model the orthotropic deck structure.

Andersson et al. (2006) analysed cables in terms of their measured dynamic properties. For main span and back-stay cables, the effect of end restrains is small and negligible, but for short cables this influence is significant. The study introduces some suggestions on how the vibration method using many frequencies of an individual cable can be used for identifying the end restrains, stiffness and forces in the cables and hangers.

Zhang et al. (2011) investigated the experimental characterization of long-span bridges by ambient vibration testing, with a particular focus on the evaluation of data quality, uncertainty reduction and data interpretation for reliable structural identification.

Apaydın et al. (2016) developed 3D FEM of the FSM Bridge using shell elements for the deck and towers and beam elements for the cables. In addition to linear dynamic analysis, a nonlinear static analysis was also conducted. Comparisons of the results with those from previous studies and ambient vibration tests showed very good agreement. Using shell elements instead of beam elements to model the deck and towers is found to be more appropriate to represent the torsional modes.

1.3. Objectives and Scope

In theory, the bridge is a single dynamic system because of the interaction among the components. However, structural elements such as deck, towers and cables show different structural behaviour and well-separated dominant frequencies. Therefore, the components can be studied independently by identifying these frequencies and separating their response from the records by using band-pass filters.

The objective of this study is to identify the forces in the main components of the bridge (i.e., main suspension cables, back-stay cables, hangers and towers), and the flexibility of the steel suspended deck from their measured dominant frequencies under different traffic loads. The results are compared to those from previous investigations (e.g., field tests, analytical models and design calculations), and are found to be consistent. The methodology is based on the theoretical formulation of the dynamic response of a suspension bridge and its components.

The scope of this study covers the definition of the bridge and the monitoring system, carried out by a detailed investigation of the structural elements frequencies and corresponding forces on structural members of the FSM Bridge as obtained from analyses of real time and temporary ambient vibration recording.

The studies which are carried out within the scope of this thesis are presented in various chapters. General outline of the bridge, design loads, structural components of the bridge and the monitoring system is presented in Chapter 2. In the next, methodology of analysis which includes data analysis, analytical expressions relating natural frequencies to forces and summary of comparisons with previous studies is evaluated in Chapter 3. Conclusions in this study are shown in Chapter 4.

2. DESCRIPTION OF THE BRIDGE AND INSTRUMENTATION

2.1. General Outline of the Bridge

FSM Bridge is a modern long span, box-girder suspension bridge. Construction of the bridge was started in 1986 and completed in 1988. The centre span of the FSM Bridge is 1090.36 m and the side spans are 210.00 m. The total length of the bridge is 1510.36 m (see, Figure 2.3). The bridge deck is a hollow box girder with orthotropic stiffeners, 3.00 m high and 39.40 m wide, with 4-lane traffic in each direction (see, Figure 2.4). The diaphragm wall panels of the deck in the transverse direction are placed at approximately every 4 m. The steel towers of the bridge are composed of rectangular box sections with heights 111.10 m above the ground level (see, Figure 2.5). The towers of the bridge are anchored at the ground level, which means that the ends of the deck are the level of the tower base. Therefore, the bridge has no approach slab. The mid-point of the deck is 64.00 m high from the sea level and the roadway at deck ends is 8.00 m above the foundation level. The rocker and expansion bearings at the deck ends allow rotations around the transverse axis but restrict rotations around longitudinal and vertical axes. Each suspension cable is connected to the bridge deck with 60 vertical hangers at 17.92 m intervals. The hangers connect to the deck and suspension cable with single hinged bearings. Table 2.1 presents detail of dimensions of the FSM Bridge.

Table 2.1. Dimensions of the FSM suspension bridge.

Structural Dimensions of The FSM Suspension Bridge							
Span Lengts				Height of Deck (m)	Deck Width (m)	Lanes (m)	Total Height of Tower (m)
Side Spans (m)	Main Span (m)	Lengt Between Anchorages (m)	Navigational Clearance (m)				
210.00	1090.36	1510.36	64.00	3.00	39.40	2x4	111.10

The deck, towers and cables have masses of 16960, 6820 and 10250 tons, respectively. The bridge was designed according to the provisions of the British Standard with some modifications according to the Japanese Industrial Standards (IHI, MHI and NKK Corp, 1989).

Figure 2.1. Location in aerial view of the FSM suspension bridge.

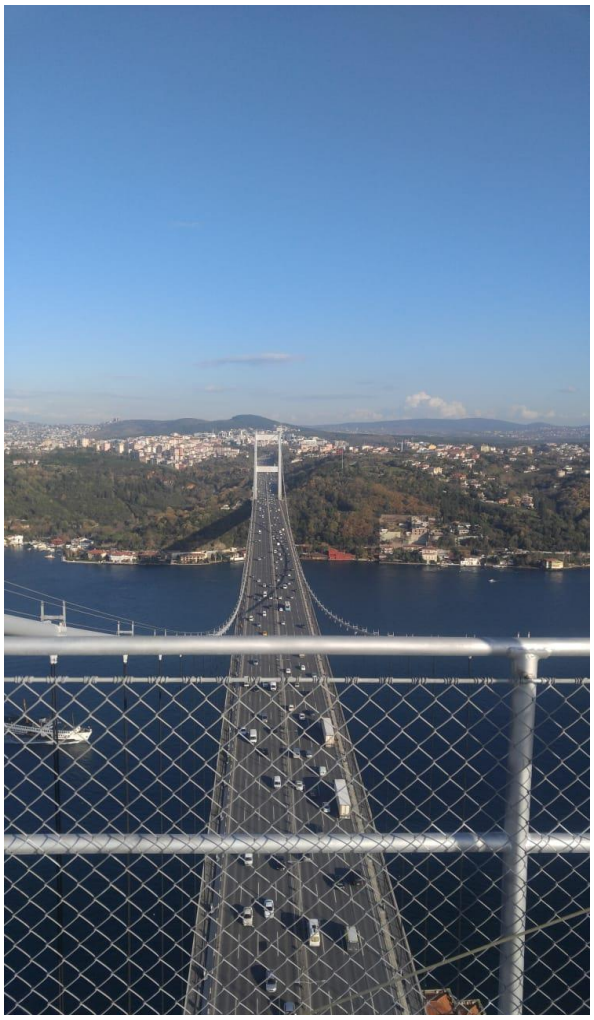

Figure 2.2. General view of the FSM suspension bridge from top of the European tower.

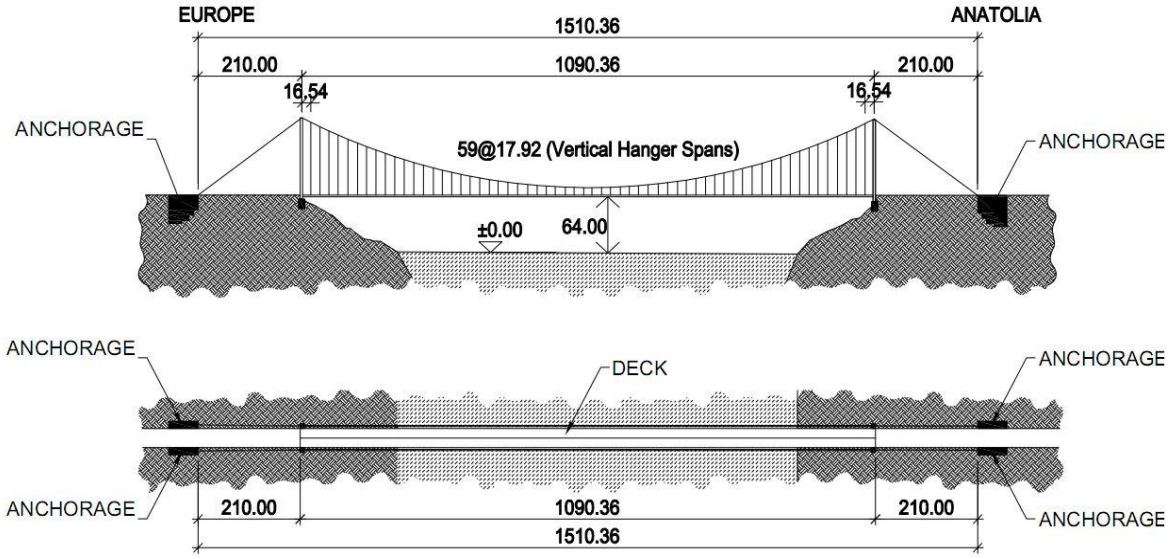

Figure 2.3. Span dimensions.

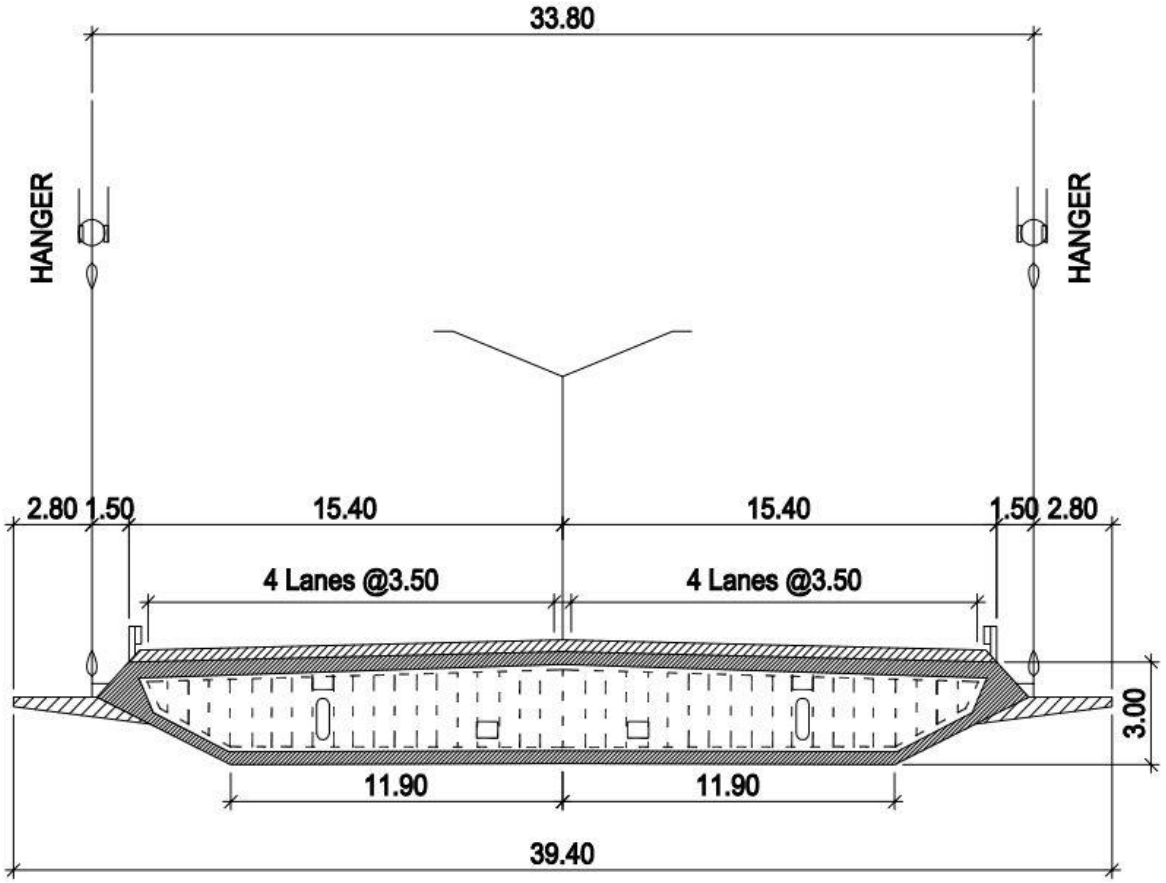

Figure 2.4. Typical deck cross section.

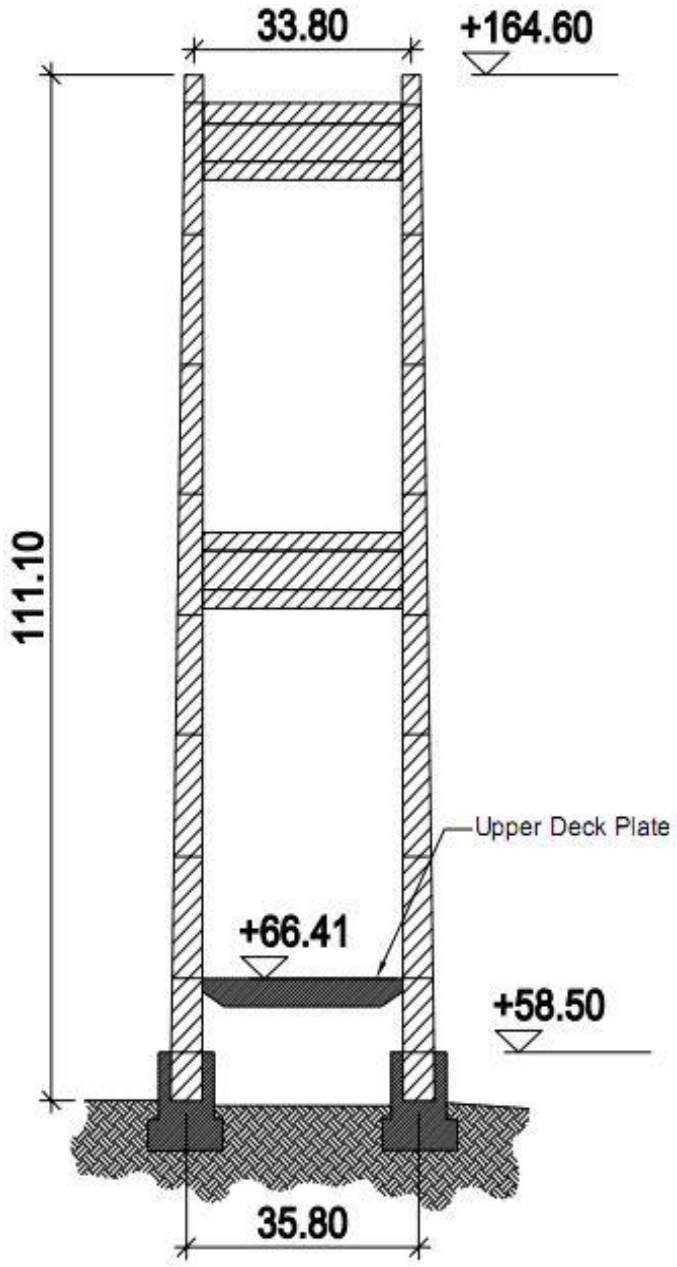

Figure 2.5. Tower dimensions and elevations.

2.2. Design Loads

Dead, live and moving loads, as well as the wind and earthquake loads considered for design are summarized below. Since the span length is more than 360 meters, a uniform lane load corresponding to H30 S24 specified in "Technical Specifications for Highway Bridges, General Directorate of Highways Turkey" was taken as 9 kN/m on truck lanes. It was assumed that two lanes (truck lanes) on both sides would be loaded by 9

kN/m uniform lane load and the other two lanes (car lanes) on both sides would be loaded by 1/3 of the uniform lane load. In addition to the uniform lane load, knife-edge load of 240 kN for truck lanes and 80 kN for car lanes were considered in calculations. According to design manual, a total design live load (LL) of the FSM Bridge considered about 8000 t.

The maximum design wind force was taken equivalent to wind gust speed of 45 m/sec (160 km/h) at deck level. Wind effects are of major importance for suspension bridges of this size. Wind tunnel tests were performed by the National Marine Institute (NMI) in England on section models of the deck to establish its aerodynamic stability. Horizontal and vertical seismic coefficients of 0.10g and 0.05g respectively were used for earthquake load in the bridge design (IHI, MHI and NKK Corp, 1989).

2.3. Structural Components of the Bridge

2.3.1. Anchorages

At both ends of the bridge there are massive reinforced concrete anchor blocks transferring the pull of the main cables into the bedrock. They are 50x60 m in plan and have a depth of 35 m. Within the anchorage blocks, there is an anchorage chamber where the cables are fixed. At the top of the anchorage chamber, the main cable splays out into 36 separate strands and each strand is fixed separately (IHI, MHI and NKK Corp, 1989).

2.3.2. Tower Foundations and Retaining Wall

The tower foundations were designed as a separate rectangular shaped massive concrete blocks and placed into the bedrock with sufficient bearing capacity. Tower foundations of the bridge are 14.00x18.00 m in plan and they have an average depth of 6.00 to 20.00 m. The bases of the towers were embedded directly into the concrete piers by approximately 5.00 m and it is assumed that there is no soil-structure interaction (IHI, MHI and NKK Corp, 1989).

2.3.3. Main Span and Back-Stay Cables

Main-span cables of the bridge were formed by aerial spinning method. The spinning wheel was carried 4 single wires at a time in a single direction. Each main cable consists of 32 strands, which extend from anchorage to anchorage with an addition of 4 thinner strands in the backstays between anchorages and main tower saddles. The main strands contain 504 wires each and the thinner strands 288 and 264 wires. The wires are 5.38 mm in diameter and of galvanized high tensile steel. In the final state, the diameter of the suspension cable in the main span is 0.77 m. The maximum suspension cable force under dead load (DL) and dead+live loads (DL+LL) at the top of the towers is 187 MN and 232.50 MN, respectively. The diameter of the back-stay cable is 0.80 m and supports an axial tensile force under DL and DL+LL loads at the top of the towers are 200.20 MN and 248.10 MN, respectively. After stretching of the cable, adjustments were made by applying tensions using strain equipment (IHI, MHI and NKK Corp, 1989).

2.3.4. Hanger Cables

Deck loads are transferred to the main cables by hangers. The cable clamps were erected along the main cables with 17.92 m intervals and tightened to the cable surface by means of rods. Vertical twin hangers were mounted to the clamps and each has a diameter of 76 mm and tensile strength of 370 tons (IHI, MHI and NKK Corp, 1989).

2.3.5. Steel Suspended Deck

The steel suspended deck is a hollow box composed of orthotropic stiffener panels with an aerodynamic cross section. The deck cross-section is 33.80 x 3.00 m and includes a cantilever side-walk of 2.80 m at each side. Total width of the deck is 39.40 m. The deck is connected to the main cables with the hangers. A-frame steel rocker bearings are used to restrict motions of the deck at the towers. At the ends of the deck, special expansion joints are used (see, Figure 2.6).

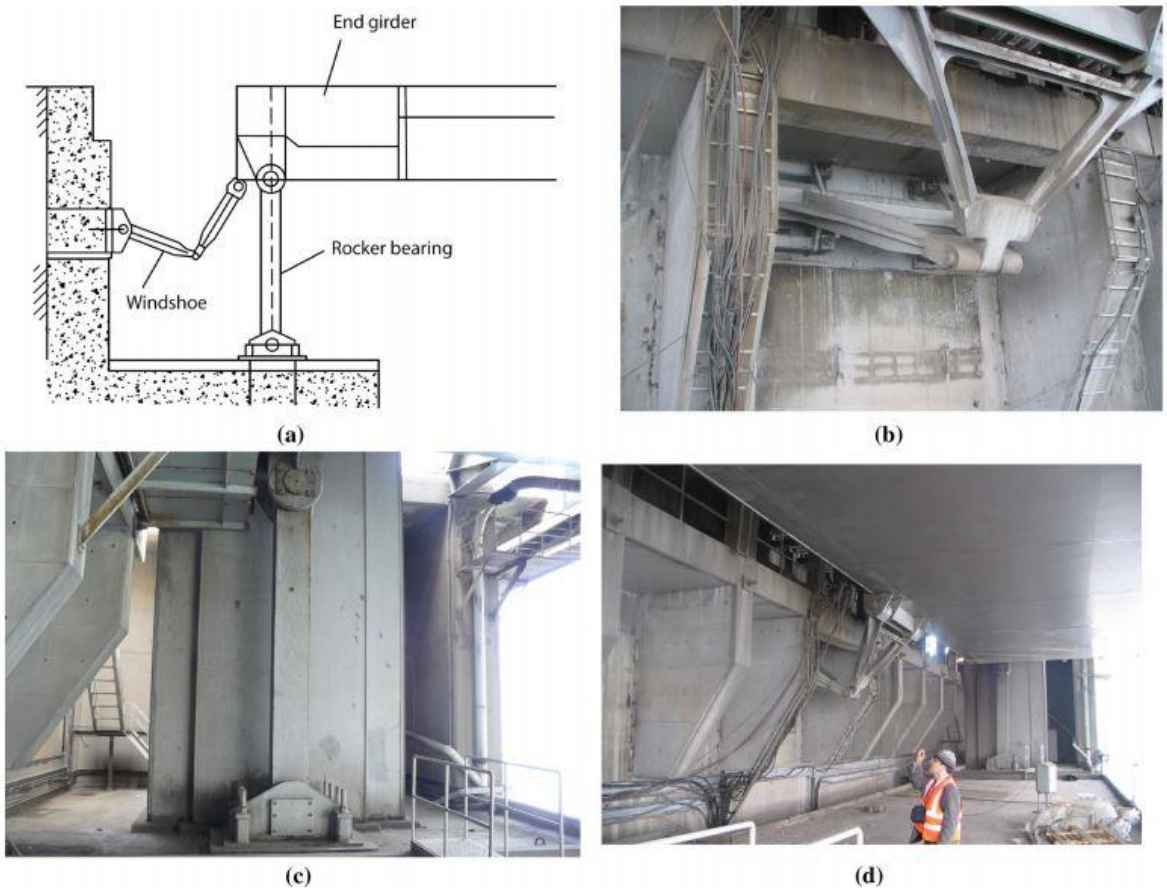

Figure 2.6. Support at the end of main span: (a) schematic view of the components, (b) wind shoe, (c) rocker bearing and (d) overall view of the end girder (Apaydın et al., 2016).

2.3.6. Steel Towers

The towers, which support the main cables of the bridge, are 111.10 m high. They were erected in 8 levels by using high yield stiffened steel panels joined with bolts at their corners. 450 tons and 650 tons cranes were used during the erection. The tower legs are 5.00x4.00 m, joined with two horizontal portal beams. Main cables are supported by saddles located on top of each tower. The maximum axial force under DL and DL+LL at the top of the both towers is 151.30 MN and 176.50 MN, respectively. (IHI, MHI and NKK Corp, 1989).

Table 2.2 and Table 2.3 present detail of material and sectional properties of the bridge.

Table 2.2. Material properties of FSM suspension bridge.

MATERIAL PROPERTIES			
Structural Element	**Density (kg/m³)**	**Young's Modulus (MPa)**	**Poisson's Ratio**
Deck	8680	210000	0.3
Tower	8680	210000	0.3
Main Cable	8530	189300	0.3
Back Stay Cable	8530	189300	0.3
Hanger Cable	8530	89100	0.3

Table 2.3. Section properties of FSM suspension bridge.

SECTION PROPERTIES				
Structural Element	**D (m)**	**A (m²)**	**Iyy (m⁴)**	**Izz (m⁴)**
Back Stay Cable	0.80	0.39129	0.01220	0.01220
Main Cable	0.77	0.36615	0.01070	0.01070
Hanger Cable	0.076	0.00506	0.000002041	0.000002041
Deck	-	1.25816	1.73180	129.273
Tower	-	1.48650	0.99290	5.0152
		1.441	0.7924	4.2921
		1.374	0.5494	3.3472
		1.3335	0.43	2.8398
		1.2751	0.2901	2.1927
		1.2029	0.1847	1.6311
		0.4699	-	3.5925
		0.3109	-	2.4191

A: Cross Sectional Area of The Element
Iyy, Izz: Moment of Inertia of the Element
D: Diameter

2.4. Instrumentation and Sensor Locations

The large physical sizes of the bridges necessitates extensive array of different sensors and appropriate technologies for data acquisition/reduction for rational health monitoring applications.

The bridge was instrumented in 2008 with 44 channels of acceleration sensors, collecting continuous data at 100 sample per seconds (see, Figure 2.13). The data are transferred in real time to the Structural Monitoring Centre at the Department of Earthquake Engineering of Kandilli Observatory and Earthquake Research Institute. The accelerometers are +/- 2.00g force-balance type accelerometers (CMG-52s by Guralp; see Figure 2.7) In addition to accelerometers; the instrumentation includes a 24-bit digitizer/recorder, communication and GPS timing modules and a power supply.

Figure 2.7. Triaxial and uniaxial strong motion accelerometers.

The data are collected continuously from the permanent sensors. For this study, measurements of ambient vibrations from additional locations were carried out on 25 October 2017. The station at the south leg of the tower in Asian side was not working. Also there are no sensors to monitor the vibrations of the back-stay and hanger cables. Therefore, temporary sensors were installed on one the back-stay cable and the longest hanger on the European side of the bridge to collect ambient vibration data on 14th of November in 2018 (see, Figure 2.8 and Figure 2.9).

Figure 2.8. Temporary seismic network installation for back-stay cable (strong motion accelerometer, transducer, power supply and laptop computer).

Figure 2.9. Temporary seismic network installation for longest hanger cable (strong motion accelerometer, transducer, power supply and laptop computer).

Figure 2.10 shows the position of sensors of the main span cables. The sensors are triaxial accelerometers measuring longitudinal, lateral and vertical vibrations at the midspan.

Figure 2.10. Permanent position of sensors on the main span cables (number 11-12).

FSM Bridge is symmetric and the side spans of the bridge do not have suspension deck. This simplifies the testing as measurements on side spans are not required and 10 stations with total of 30 channels to measure the ambient vibration response through the deck. Figure 2.11 illustrates the number 10 sensor located on 1/10 of the span from Europe to Asia side of the deck.

Figure 2.11. Permanent sensor inside the deck (number 10).

Figure 2.12 represents the sensor installation on top of the European-side tower, South leg and station has two channels to measure the ambient vibration response of the tower like the other legs. The location of station has been determined to get the most of the lateral modes as well as mode shapes of the relevant modes appropriately.

Figure 2.12. Permanent sensor inside the Europe tower, South leg (number 16).

The specific locations and directions of the permanent sensors in the bridge are presented in Table 2.4 and Figure 2.13.

Table 2.4. Specific locations of the permanent sensors on the bridge.

LOCATIONS OF THE SENSORS		
SENSOR	**TYPE OF MOTION**	**LOCATION ON THE BRIDGE**
1	Longitudinal, Lateral, Vertical	1/10 of the span, from Asia to Europe side of the girder
2	Longitudinal, Lateral, Vertical	2/10 of the span, from Asia to Europe side of the girder
3	Longitudinal, Lateral, Vertical	3/10 of the span, from Asia to Europe side of the girder
4	Longitudinal, Lateral, Vertical	4/10 of the span, from Asia to Europe side of the girder
5	Longitudinal, Lateral, Vertical	5/10 of the span, from Asia to Europe side of the girder
6	Longitudinal, Lateral, Vertical	6/10 of the span, from Asia to Europe side of the girder
7	Longitudinal, Lateral, Vertical	7/10 of the span, from Asia to Europe side of the girder
8	Longitudinal, Lateral, Vertical	8/10 of the span, from Asia to Europe side of the girder
9	Longitudinal, Lateral, Vertical	9/10 of the span, from Asia to Europe side of the girder
10	Longitudinal, Lateral, Vertical	10/10 of the span, from Asia to Europe side of the girder
11	Longitudinal, Lateral, Vertical	5/10 of the span, midsag Main Cable in the North
12	Longitudinal, Lateral, Vertical	5/10 of the span, midsag Main Cable in the South
13	Longitudinal, Lateral	Top of the Asia Tower, North Leg
14	Longitudinal, Lateral	Top of the Asia Tower, South Leg
15	Longitudinal, Lateral	Top of the Europe Tower, North Leg
16	Longitudinal, Lateral	Top of the Europe Tower, South Leg

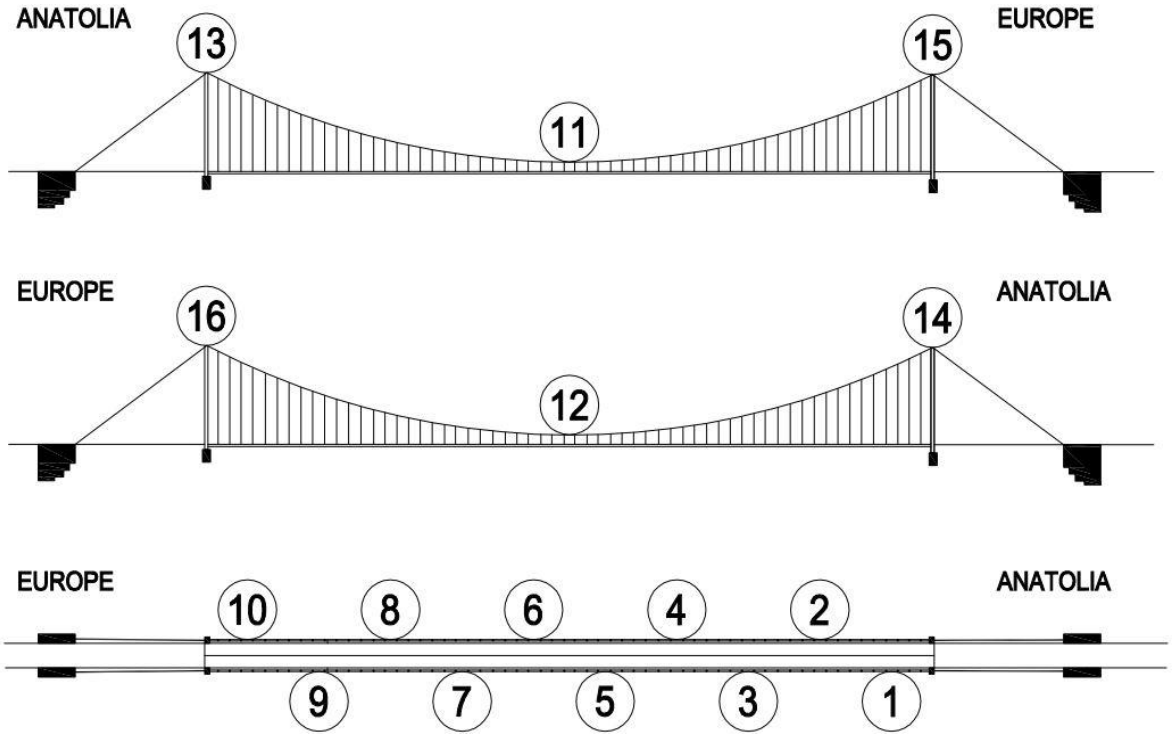

Figure 2.13. The layout of the permanent seismic network installation system on the bridge.

2.5. Data Acquisition

Data collection involves gathering and measuring signals from sources and digitizing the signals. The ambient vibration data collected from Structural Health Monitoring (SHM) systems are in discrete time domain. The same information can be expressed in frequency domain. Data are recorded at 100 Hz. The sensors are synchronized by using a GPS time antenna in the monitoring system. The continuous records are archived in 24 hour-long files. The record length from the additional temporary sensors installed for this study was 30 minutes.

3. METHODOLOGY OF ANALYSIS AND DISCUSSION OF RESULTS

3.1. Data Analysis

The dominant frequencies of the components are identified from the spectral analysis of the records. The records are first processed by applying baseline corrections, de-trending and band-pass filtering. The Fast Fourier Transform (FFT) of the processed records are smoothed by using triangular smoothing windows with optimum lengths to identify the resonant frequencies.

The variations in the dominant frequencies of structural members for heavy and light traffic conditions are identified and the corresponding member forces are calculated. The results are compared with those of the previous ambient vibration surveys and finite element models.

The analysis in this study is based on the data from ambient vibrations of the bridge, generated by traffic and wind loads. Ambient vibration records are generally small amplitude signals with low Signal-to-Noise-Ratio (SNR). However, this kind of data also presents some advantages. The main advantage is the records are infinitely long and always available. There is no need to wait for an earthquake, or utilize some sort of external excitation for analysis. Infinitely-long data allow the utilization of statistical signal-processing tools, which are very powerful to reduce the noise in the records. Moreover, ambient vibration data, in general, represent the linear response of the structure and the recorded vibration signals are stationary (i.e., their time and frequency domain properties do not change with time).

Raw data from the sensors were collected and saved in *.gcf format (i.e., the format of the sensor manufacturer) and then converted into the American Standard Code for Information Interchange (ASCII) (*.txt) format. These files were then organized on a single computer. Raw data do not provide a good identification of the dynamic properties of the structure because of the noise in the data, imperfetions in the instruments,

installation problems and the environmental conditions. Thus, the data must be processed before analyzing it. Data processing include removal of mean, removal of linear trends, decimation, smoothing and band-pass filtering.

In this study, the processed ambient vibration data were analysed by using Fourier-based and averaged spectral analysis techniques. The acceleration records are divided into 600-second long segments for averaging. The records are de-trended for the removal of mean and linear trends and band-pass filtered to remove unwanted high and low frequency components. The frequency range of members' vibrations was considered carefully when selecting the high-pass corner frequency of the band-pass filters.

A high-pass filter with a corner frequency of 0.15 Hz was used for the vertical vibration records of the main-span cables whereas; a high-pass filter with a corner frequency of 0.12 Hz was used for the vertical vibrations of the deck. For the lateral vibrations of the towers, the high-pass filter corner was 0.29 Hz. For the back-stay cables and the hangers, the high-pass filter corners were 0.56 Hz and 1.60 Hz, respectively.

To further reduce the noise effects, the calculated Fourier Amplitude Spectra (FAS) were smoothed by using triangular smoothing windows. The optimum window lengths were calculated by using the methodology suggested in Şafak (1997). Spectral analyses of the records from main-span cables, the deck and towers are conducted for heavy and light traffic conditions. However, back-stay and hanger cables are performed for normal traffic condition. All calculations were carried out by using the MATLAB R2018b software program.

3.2. Analytical Expressions Relating Natural Frequencies to Forces of the Bridge Members

The classical method for SHM and system identification of suspension bridges is to install sensors on structural elements of the bridge (e.g., cables, deck and the towers) and analyse the records to identify modal properties, such as the modal frequencies, damping ratios and mode shapes of the bridge. Usually, FEM of the bridge is then calibrated by matching the identified modal parameters.

Due to their large size, geometric nonlinearities, non-proportional damping and moving traffic loads, most suspension bridges do not meet the requirements and assumptions of classical modal analysis. Also, since there are an infinite number of modes, it is not possible to identify all of them and to develop a single model that match the recorded data.

The main components of a suspension bridge are the suspension cables, towers, the deck and the hangers that connect the deck to the suspension cables. Theoretically, the bridge is a single dynamic system because of the interaction among the components. However, due to the differences in their flexibilities and the degrees of freedom, the response of some of the components can be studied independently by separating the frequency bands in the records (i.e., by using band-pass filters) that are pertinent only to the vibrations of that component.

There are several experimental and analytical studies done in the past for the FSM Bridge. Brownjohn et al. (1992) performed a detailed ambient vibration survey. Dumanoglu et al. (1992) carried out 2D and 3D FEM of the bridge to examine different types of modes using beam elements. Apaydın et al. (2016) developed a more detailed 3D FEM using thin shell elements for the towers and the deck. The model was created directly from the design drawings of the bridge.

It was found from the finite element studies that lateral and vertical motions of the deck are well correlated with those of the main span cables and the lateral and longitudinal motions of the towers. The lateral and longitudinal motions of the towers also control the motions of the back-stay cables.

On a normal day, no ambient vibration data can be obtained under pure DL because of the traffic loads. Therefore, the frequencies and the forces under DL are approximated from the data collected after midnight under very light traffic condition. The frequencies and forces under DL+LL condition are approximated from the data collected during rush hour (heavy traffic condition). The SHM system on the bridge did not include any sensors on the back-stay cables and hangers. The vibrations of these components are recorded by using portable sensors during the day under normal traffic conditions.

According to the design manual of the bridge, design moving load is about 8000 tons, as stated in Section 2.2. Therefore, forces on members obtained under pure DL are only calculated when the value of the LL is taken as zero. However, structural member forces under DL+LL are calculated in this study when design LL is taken as 8000 tons.

In the following sections, the analytical expressions for each main component of the bridge are presented. Forces on the members are estimated from their dominant frequencies by using analytical expressions. The results are compared with those from the finite element study by Apaydın (2002) and the record book of the bridge by the contractors (IHI, MHI and NKK Corp, 1989). Good agreement is found between this and the other two studies.

3.2.1. Cables

The identification of cable force based on vibration measurements has first been proposed by Mars and Hardy (1985) based on the observation on the cables and hangers of cable-stayed and bowstring bridges. The basis for this methodology is the dynamic equilibrium equation of a tensioned beam. The accuracy of the estimated cable force depends primarily on the physical parameters of the cable, such as the cross-sectional area, elasticity modulus, moment of inertia and the mass per unit length. Mars and Hardy suggested different models based on the boundary conditions and cable properties.

3.2.1.1. Main Span Cables

Analytical expressions:

The two main suspension cables can be modeled as an elastic cable with uniform cross section subjected to axial tension H and a uniformly distributed vertical load p as shown in Figure 3.1. The vertical load p represents the sum of the cable weight plus the weight of the deck and the hangers. When held at the same elevation at both ends, such cables sag into a catenary, whose vertical profile can be expressed analytically in the form of a hyperbolic cosine functions. For shallow catenaries, where $L/d>8$ (Figure 3.1), the

axial tension in the cable is approximately constant and the vertical profile *w(x)* can be approximated by a shallow parabola, as given below (Timoshenko et al., 1965):

$$w(x) = \frac{pL^2}{2H}\left[\frac{x}{L} - \left(\frac{x}{L}\right)^2\right] \tag{5.1}$$

where, L is the span length.

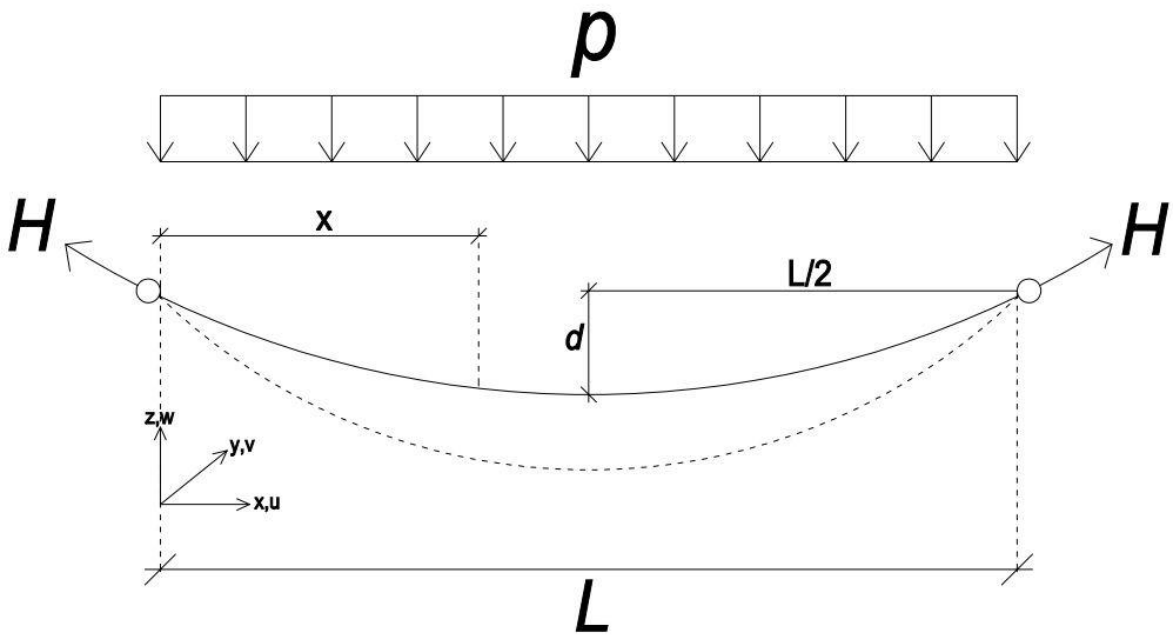

Figure 3.1. Notation and the loads for the cables.

for a parabolic catenary, the main span cable length with sag, L_e, is:

$$L_e = \int_o^L \left(\frac{ds}{dx}\right)^3 dx \rightarrow L_e \approx L.\left[1 + 8\left(\frac{d}{L}\right)^2\right] \tag{5.2}$$

the maximum midspan sag, d is:

$$d = \frac{pL^2}{8H} \tag{5.3}$$

the measure of sag is defined by the following parameter, α^2 as given below:

$$\alpha^2 = \left(\frac{8d}{L}\right)^2 \frac{EA}{H}\frac{L}{L_e} \tag{5.4}$$

where, E is the modulus of elasticity and A is the cross sectional area of the main span cable. The parameter α^2 is of fundamental importance in the static and dynamic response of suspended cables. Basically the parameter accounts for the geometric and elastic effects. Non-dimensional frequency parameter, λ_c, is found by solving the following equation:

$$tan\left(\frac{\pi\lambda_c}{2}\right) = \frac{\pi\lambda_c}{2} - \frac{4}{\alpha^2}\left(\frac{\pi\lambda_c}{2}\right)^3 \tag{5.5}$$

In Table 3.1, the frequencies of the first eight symmetric in-plane modes are tabulated for a wide range of values of the parameter involving cable elasticity and geometry.

Assuming that, the cable profile is a shallow catenary, longitudinal (i.e., x direction in Figure 3.1) components of the motion are negligible and the second order terms can be neglected. The natural frequencies of the cable can be calculated from the following equations (Irvine, 1981 and Abdel-Ghaffar, 1976). In vertical-plane, symmetric mode:

$$f_c = \frac{\lambda_c}{2L}\sqrt{\frac{H}{m}} \tag{5.6}$$

where f_c is natural frequency of the c^{th} mode in Hz.

Table 3.1. Relationship between λ_c and α^2.

α^2	λ_1	λ_2	λ_3	λ_4	λ_5	λ_6	λ_7	λ_8
∞	2.86	4.92	6.94	8.95	10.96	12.97	14.97	16.98
$256\pi^2$	2.86	4.91	6.93	8.93	10.93	12.91	14.81	16.00
$196\pi^2$	2.85	4.91	6.92	8.92	10.91	12.81	14.00	15.15
$144\pi^2$	2.85	4.90	6.91	8.90	10.81	12.00	13.15	15.05
$100\pi^2$	2.85	4.89	6.89	8.80	10.00	11.15	13.04	15.02
$64\pi^2$	2.84	4.87	6.79	8.00	9.14	11.04	13.02	15.01
$36\pi^2$	2.82	4.78	6.00	7.14	9.04	11.02	13.01	15.01
$16\pi^2$	2.74	4.00	5.12	7.03	9.01	11.01	13.00	15.00
100	2.60	3.48	5.05	7.01	9.01	-	-	-
80	2.48	3.31	5.04	7.01	9.01	-	-	-
60	2.29	3.18	5.03	7.01	-	-	-	-
$4\pi^2$	2.00	3.09	5.02	7.01	-	-	-	-
20	1.61	3.04	5.01	7.00	-	-	-	-
10	1.35	3.02	5.00	-	-	-	-	-
8	1.23	3.01	-	-	-	-	-	-
6	1.22	-	-	-	-	-	-	-
4	1.15	-	-	-	-	-	-	-
2	1.08	-	-	-	-	-	-	-
1	1.04	-	-	-	-	-	-	-
0	1.00	-	-	-	-	-	-	-

Records and frequencies identified:

Figures below show recorded acceleration-time histories and Smoothed Fourier Amplitude Spectra (SFAS) of main span cables in vertical direction under light and heavy traffic conditions.

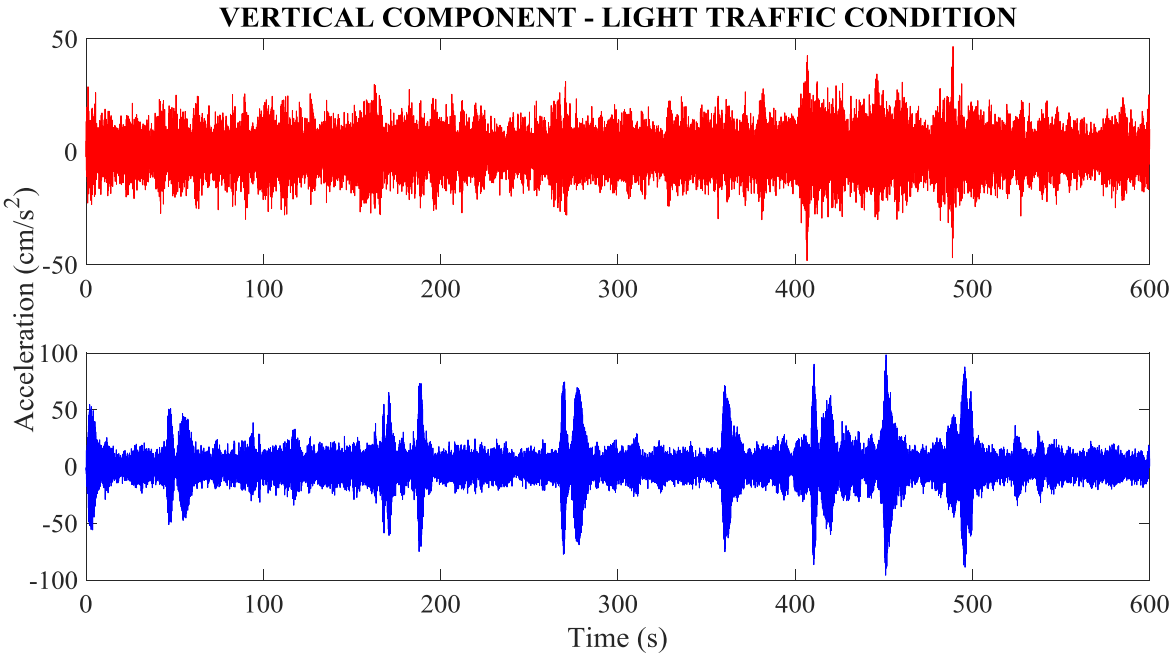

Figure 3.2. Recorded acceleration-time histories for light traffic condition in vertical direction of the main span cables (location 11-12 respectively).

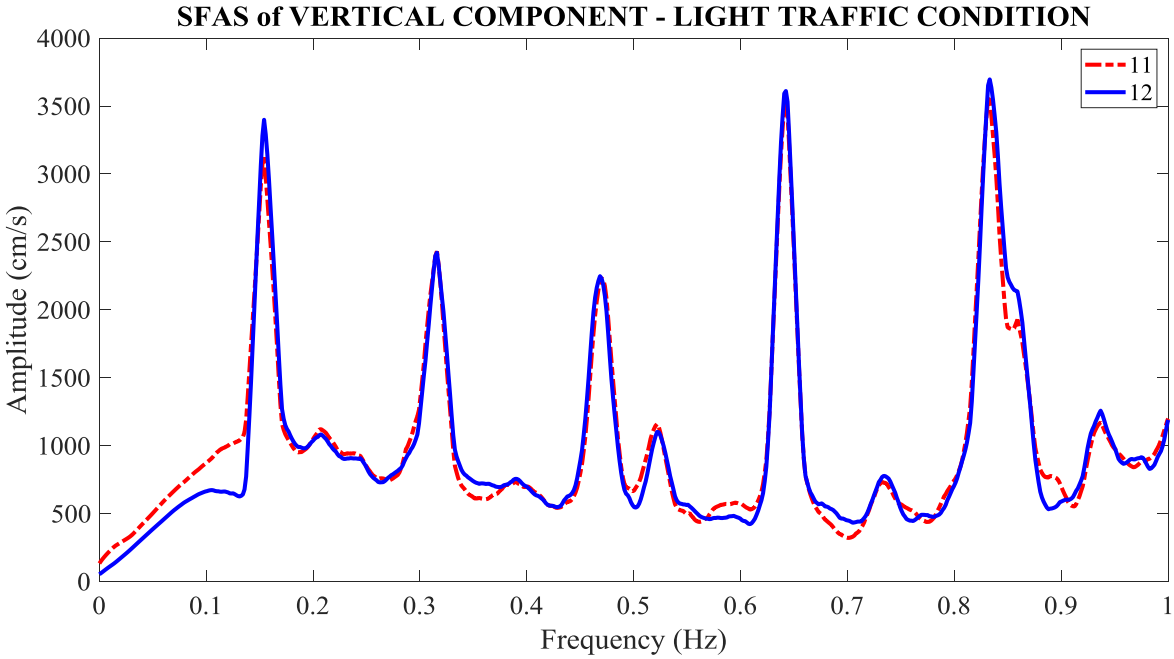

Figure 3.3. SFAS at light traffic condition in vertical direction of the main span cables.

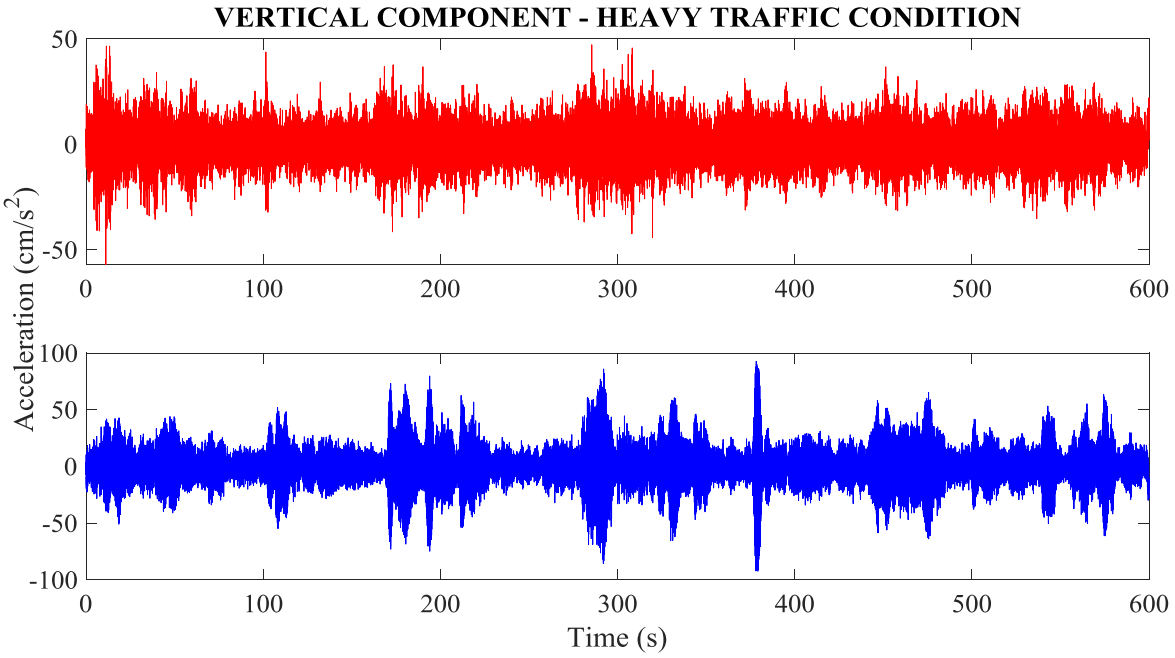

Figure 3.4. Recorded acceleration-time histories for heavy traffic condition in vertical direction of the main span cables (location 11-12 respectively).

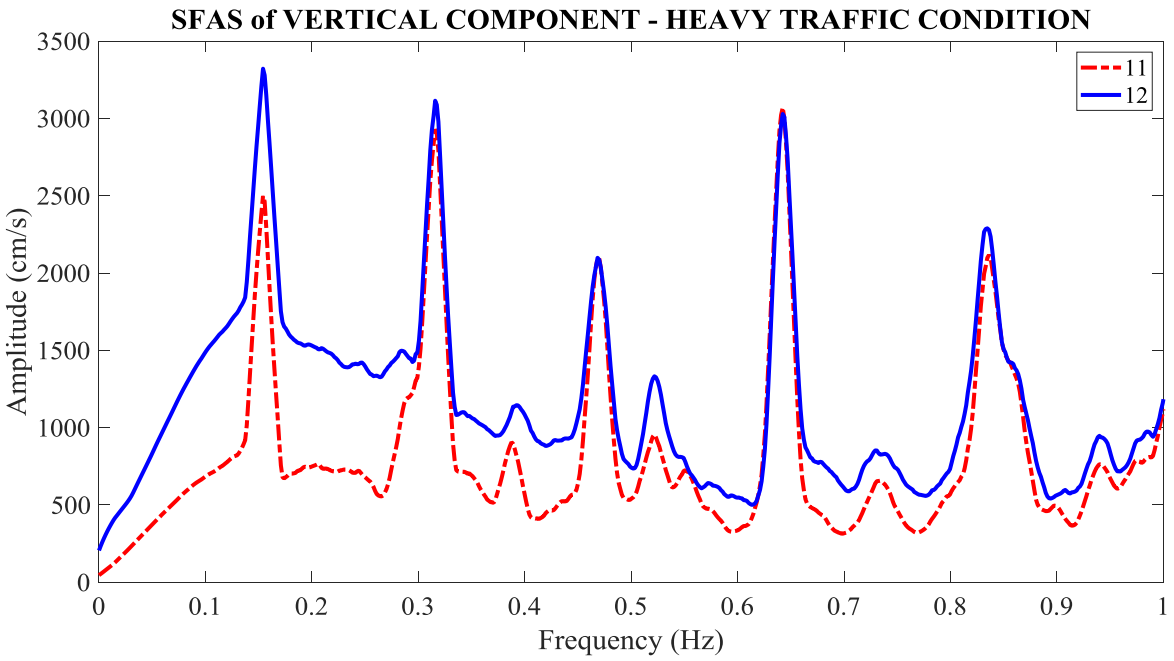

Figure 3.5. SFAS at heavy traffic condition in vertical direction of the main span cables.

The resonant frequencies shown in Figure 3.3 and Figure 3.5 are tabulated on Table 3.2, listing the frequencies at light and heavy traffic conditions for the vertical vibrations of the main span cables. No previous studies are available for comparison.

Table 3.2. Mode frequencies in vertical direction of the main span cables.

Ambient Vibration Survey of the FSM Suspension Bridge		
Kavak (2019)		
Vertical Main Cable Modes	**Experimental Frequency (Hz)**	
	Light Traffic Condition	**Heavy Traffic Condition**
MCV1	0.1541	0.1526
MCV2	0.3159	0.3159
MCV3	0.4700	0.4684
MCV4	0.5219	0.5203
MCV5	0.6424	0.6424
MCV6	0.7339	0.7324
MCV7	0.8331	0.8316

Calculated forces:

the tension force on the main span cable under DL:

$d \approx 97.20\ m$

$E = 189300.00\ MPa = 19303227.00\ tons/m^2$ (Table 2.2)

$A = 0.36615\ \text{m}^2$ (Table 2.3)

from Equation 5.2:

$$L_e = 1090.36\left[1 + 8\left(\frac{97.20}{1090.36}\right)^2\right] = 1159.68\ m$$

assume as $m_{LiveLoad} = 0.00$ tons:

$$m = \left[\left(m_{Deck} + m_{Main+HangerCables} + m_{LiveLoad}\right)/(g\ x\ L)\right]/2$$

$$m = [(16960.00\ +\ 7085.06\ +\ 0.00)/(9.81\ x\ 1090.36)]/2 = 1.124\ \text{tons.s}^2/\text{m}^2$$

from Equation 5.4:

$$\alpha^2 = \left(\frac{8\ x\ 97.20}{1090.36}\right)^2 \left(\frac{19303227\ x\ 0{,}36615\ x\ 1090.36}{16685.67\ x\ 1159.68}\right) = 202.56$$

$\alpha^2 \rightarrow 202.56\ as\ \lambda_1 \rightarrow 2.758$ (Table 3.1)

$f_1 =$ 0.1541 Hz (*1st* mode frequency under light traffic condition in Table 3.2)

from Equation 5.6:

$$0.1541 = \frac{2.758}{2\ x\ 1090.36}\sqrt{\frac{H}{1.124}} \rightarrow H = 16685.67\ tons$$

tension force under DL+LL (assume as $m_{LiveLoad} = 8000.00$ tons):

$$m = \left[\left(m_{Deck} + m_{Main+HangerCables} + m_{LiveLoad}\right)/(g\ x\ L)\right]/2$$

$$m = [(16960.00\ +\ 7085.06\ +\ 8000.00)/(9.81\ x\ 1090.36)]/2$$

$$m = 1.498\ \text{tons.s}^2/\text{m}^2$$

from Equation 5.4:

$$\alpha^2 = \left(\frac{8\ x\ 97.20}{1090.36}\right)^2 \left(\frac{19303227\ x\ 0{,}36615\ x\ 1090.36}{22361.44\ x\ 1159.68}\right) = 151.15$$

$\alpha^2 \rightarrow 151.15\ as\ \lambda_1 \rightarrow 2.724$ (Table 3.1)

$f_1 = 0.1526$ Hz (*1st* mode frequency under heavy traffic condition in Table 3.2)

from Equation 5.6:

$$0.1526 = \frac{2.724}{2\ x\ 1090.36}\sqrt{\frac{H}{1.498}} \rightarrow H = 22361.44\ tons$$

According to the calculations above, the main span cable force under DL and DL+LL is 163.63 MN (16685.67 tons) and 219.29 MN (22361.44 tons), respectively.

It was found from analytical study that each main span cable has 165.05 MN and 229.25 MN tension force under DL and DL+LL conditions, respectively. Thus, the relative difference is about 1% and 5% under DL and DL+LL conditions.

According to the record book of the bridge, each main span cable is subjected to 187.00 MN and 232.50 MN tension force under DL and DL+LL conditions. When compared to the results of this study, the relative difference is about 12% and 6% under DL and DL+LL conditions, respectively.

3.2.1.2. Back-Stay Cables

Analytical expressions:

Backstay cables are the cables spanning between the pylon tops and the ground anchorages at both ends of the bridge. These sections do not include hangers. The back-stay cable sag is about 0.90 m.

Figure 3.6 shows the sketch of a typical backstay cable and the notations and dimensions. The distributed load, $p=mg$, represents the weight of the cable, where m is the cable mass per unit length, g is the gravitational acceleration and L represents span length.

It is assumed that the back-stay cable behaviour can be modelled as a first-order linear behaviour with uniform cross-section subjected to axial tension H_b. Note that H_b is different than H because of the different angles of slope with respect to the pylon, and the friction between the cable and the saddle at the top of the pylon.

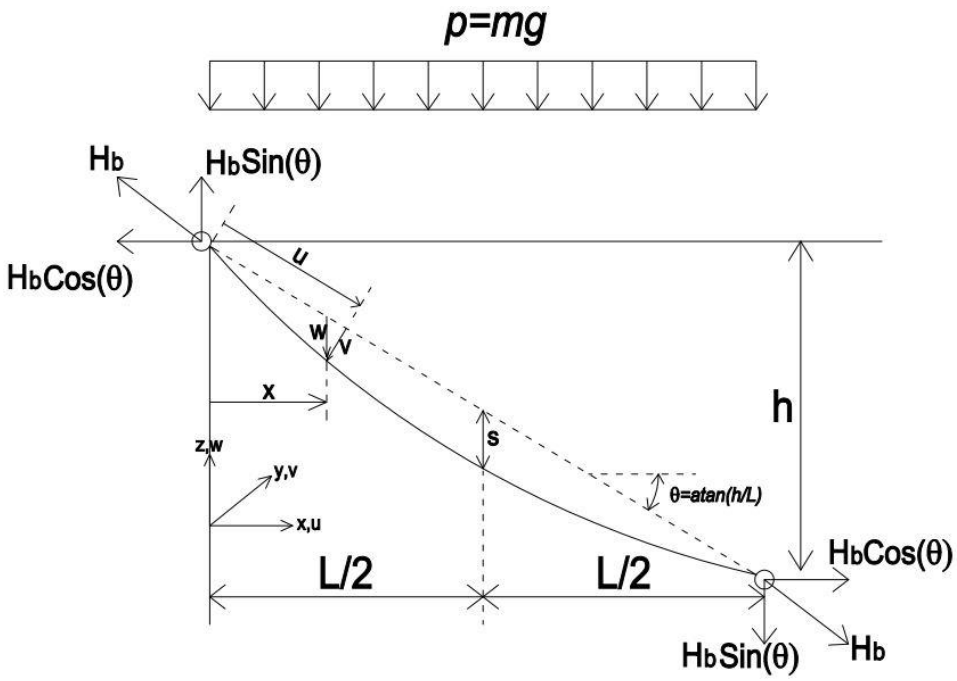

Figure 3.6. Sketch and the notation for a backstay cable.

By using the notation in Figure 3.6, the following equations can be written for the backstay cables (Timoshenko and Young, 1695):

the static configuration:

$$w(x) = \frac{mgx}{2H_b\, cos(\theta)}(L - x) + \frac{h}{L}x \tag{5.7}$$

the back-stay cable sag at mid-point:

$$s = \frac{mgL^2}{8H_b\, cos(\theta)} \tag{5.8}$$

the length of back-stay cable with sag:

$$L^* = L/\cos(\theta) \tag{5.9}$$

$$L_s = \int_{x=0}^{L} \sqrt{1 + (dw/dx)^2}\,dx \approx L^*\left(1 + \frac{8s^2}{3L^{*2}}\right) \tag{5.10}$$

the elongation of the cable:

$$\Delta L = \frac{H_b L}{AE}\left(1 + \frac{16s^2}{3L^2}\right) \tag{5.11}$$

the corresponding change in sag:

$$\Delta s = \frac{3H_b L^2}{16sAE}\left(1 + \frac{16s^2}{3L^2}\right) \tag{5.12}$$

where α^2 for back-stay cable is defined as:

$$\alpha^2 = \frac{mgL^2}{H_b^2}\left(\frac{EA}{8H_b^2 + (mgL)^2}\right) \tag{5.13}$$

where, E is the modulus of elasticity and A is the cross sectional area of the back-stay cable. The parameter α^2 accounts for the geometric and elastic effects. Non-dimensional frequency parameter, λ_c, is shown in Equation 5.5.

The relationship between α^2 and λ_c for the first eight symmetric in-plane modes is shown in Table 3.1.

The natural frequencies of the in-plane and out-of-plane vibrations of a backstay cable can be estimated from the below equation (Irvine, 1981 and Abdel-Ghaffar, 1976). In vertical-plane, symmetric mode:

$$f_c = \frac{\lambda_c}{2L^*}\sqrt{\frac{H_b}{m}} \tag{5.14}$$

where, f_c is natural frequency of the c^{th} mode in Hz.

For taut flat cables $\alpha^2 << 1$ hence, the classical linear theory of the taut string is valid. When $\alpha^2 >> 1$, the results correspond to those of the main suspension cables.

According to the flat taut string theory, both flexural rigidity and sag-extensibility of the cables are neglected. Given the measured frequency and the mode number, the computation of tension force is straightforward, and can be considered as the first approximation of the tension force. The application of this formula is strictly limited to a flat long slender cables (suspension cable), because it does not consider the bending stiffness and sag-extensibility of cables.

Considering a simply supported beam subjected to an axial tension *H*, its transverse displacement *y(x,t)* is a function of axial coordinate *x* and time *t*. Under free vibration, the equation of motion for this system can be expressed as:

$$m\frac{\partial^2 y(x,t)}{\partial t^2} - H\frac{\partial^2 y(x,t)}{\partial x^2} + EI\frac{\partial^4 y(x,t)}{\partial x^4} \tag{5.15}$$

where, *I* represents the moment of inertia of the section. It should be noted that a uniform cross section, i.e., a constant value for EI, is assumed to obtain Equation 5.15. With the given boundary conditions, an analytical formula for the modal frequencies of this model can be solved from Equation 5.15 (Humar, 1990). Equation 5.16 gives the relation between the cable force and the frequency.

$$H = 4mL_s^2\left(\frac{f_c}{c}\right)^2 - \frac{EI}{L_s^2}(c\pi)^2 \tag{5.16}$$

where L_s is the beam length with sag, f_c denotes the c^{th} natural frequency in Hz and *c* refers to mode number of cable.

Record and frequencies identified:

Figures below represent recorded acceleration-time histories and SFAS of back-stay cable in vertical direction under normal traffic condition.

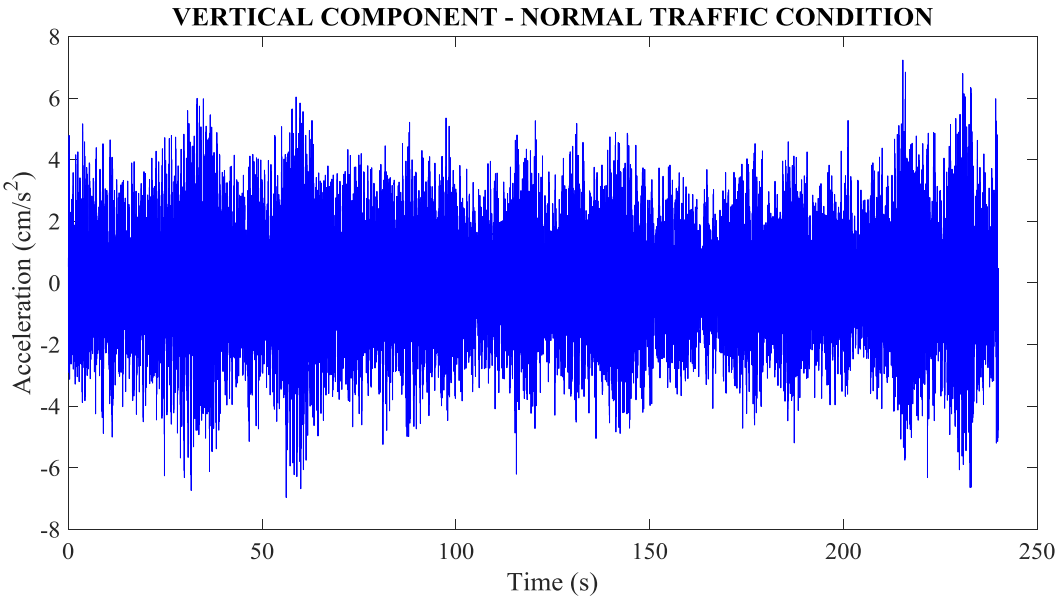

Figure 3.7. Recorded acceleration-time histories for normal traffic condition in vertical direction of the back-stay cable.

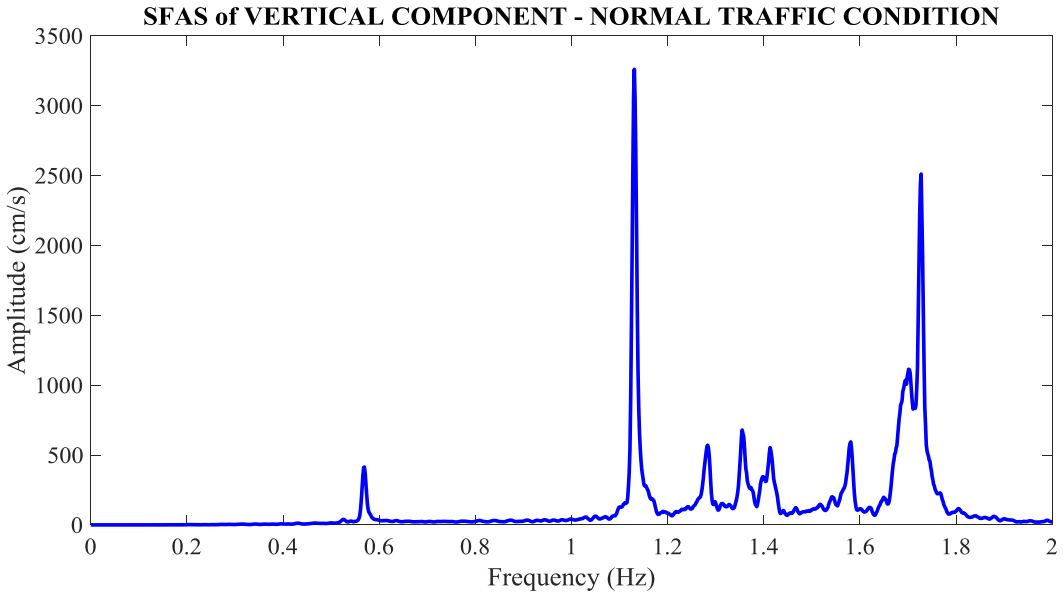

Figure 3.8. SFAS at normal traffic condition in vertical direction of the back-stay cable.

Table 3.3 lists the identified frequencies from Figure 3.8 of the back-stay cable in vertical direction under normal traffic condition. There were no results from previous studies for comparison.

Table 3.3. Mode frequencies in vertical direction of the back-stay cable.

Ambient Vibration Survey of the FSM Suspension Bridge	
Kavak (2019)	
Vertical Back-Stay Cable Modes	**Experimental Frequency (Hz)**
	Normal Traffic Condition
BCV1	0.569
BCV2	1.131
BCV3	1.283
BCV4	1.355
BCV5	1.413
BCV6	1.581
BCV7	1.727

Calculated force:

the tension force on the back-stay cable under normal traffic condition:

$\theta = arctan(110.00/210.00) = 27.646$

$E = 189300.00\ MPa = 19303227.00\ tons/m^2$ (Table 2.2)

$A = 0.39129\ m^2$ (Table 2.3)

from Equation 5.9 and 5.10:

$L^* \approx L_s = 210.00/cos\ (27.646) = 237.06\ m$

$$m = \left[\left(m_{Back-StayCables}\right)/(g\ x\ L^{*})\right]/4$$

$$m = [(3164.94)/(9.81\ x\ 237.06)]/4 = 0.34023\ tons.s^2/m^2$$

from Equation 5.13:

$$\alpha^2 = \frac{0.34023\ x\ 9.81\ x\ 210.00^2}{21386.24^2}\left(\frac{19303227\ x\ 0{,}39129}{8\ x\ 21386.24^2\ x\ (0.34023\ x\ 9.81\ x\ 210.00)^2}\right)$$

$\alpha^2 \approx 0, \quad \alpha^2 \to 0\ as\ \lambda_1 \to 1$ (Table 3.1)

$f_i = 0.569\ Hz$ (1^{st} mode frequency under normal traffic condition in Table 3.3)

from Equation 5.14:

$$0.569 = \frac{1.00}{2\ x\ 237.06}\sqrt{\frac{H_b}{0.34023}} \rightarrow H_b = 24779.08\ tons$$

The tension force on the back-stay cable, calculated under normal traffic conditions, is 243.00 MN (24779.08 tons). This value is slightly higher than that of the analytical model (239.32 MN) and the record book of the bridge (248.10 MN). The differences can be attributed to the moving loads.

3.2.1.3. Hanger Cables

Analytical expressions:

Hangers have a significant effect on the higher-mode frequencies and the flexibility of suspension bridges when the deck is stiff. For hangers with $L_h/D > 100$, where L_h is the free hanger length and D is the hanger diameter, the hangers can be assumed to behave like a taut string. For a taut string, the relationship between the hanger force and the modal frequency, is given by the following equation (Irvine, 1981 and, Gerardin and Rixen, 1997):

$$f_c = \frac{c}{2L_h}\sqrt{\frac{N_h}{m}} \tag{5.17}$$

where, f_c is c^{th} modal frequency in Hz, c is mode number and m is hanger mass per unit length.

Record and frequencies identified:

Figures below indicate the recorded acceleration-time histories and the corresponding SFAS for the longest hanger in lateral direction under normal traffic conditions.

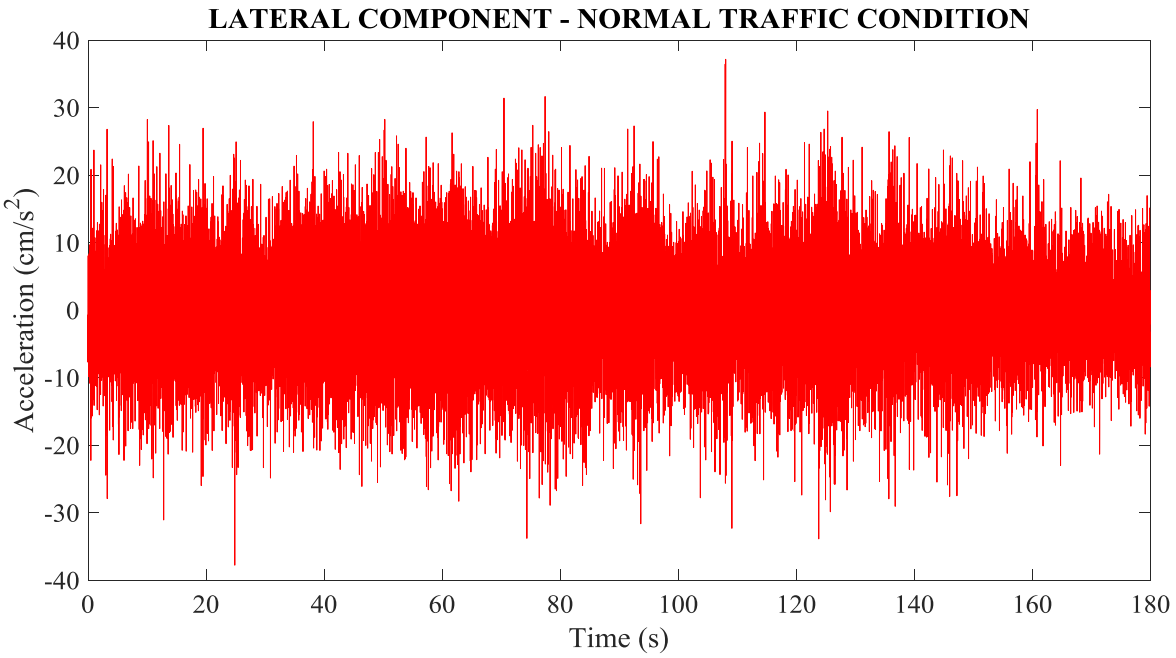

Figure 3.9. Recorded acceleration-time histories for normal traffic condition in lateral direction of the longest hanger cable.

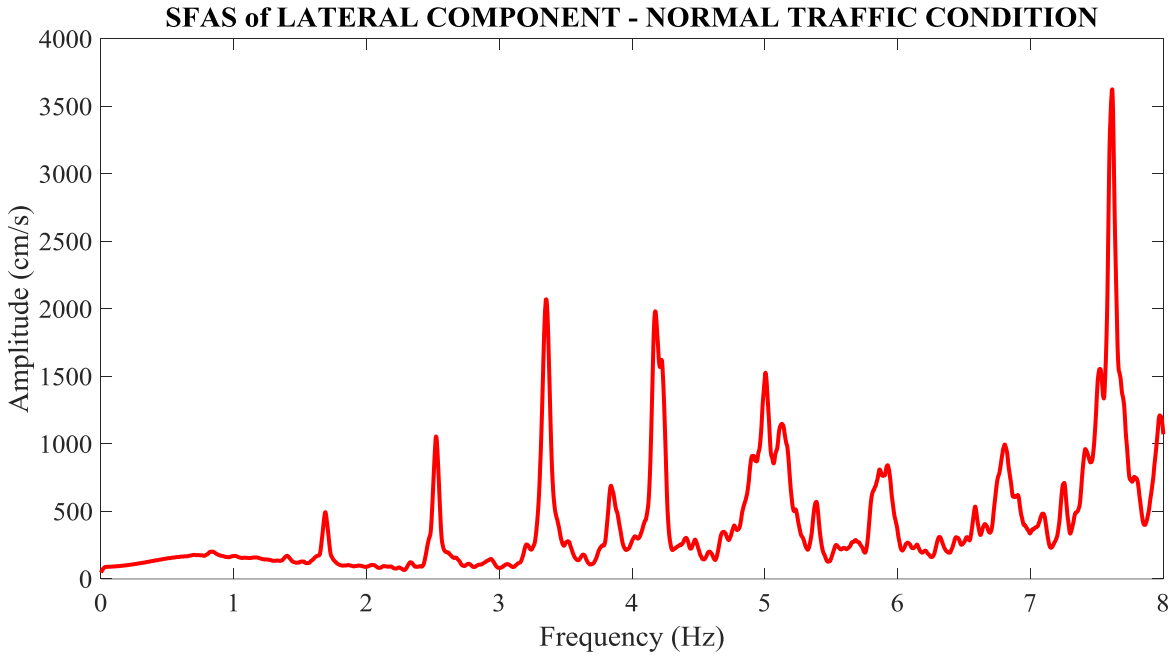

Figure 3.10. SFAS at normal traffic condition in lateral direction of the longest hanger cable.

Table 3.4 forms the frequencies in lateral direction of the longest hanger, identified from Figure 3.10 at normal traffic conditions. No such information is available from previous studies for comparison.

Table 3.4. Mode frequencies in lateral direction of the longest hanger cable.

Ambient Vibration Survey of the FSM Suspension Bridge	
Kavak (2019)	
Lateral Hanger Cable Modes	**Experimental Frequency (Hz)**
	Normal Traffic Condition
HCL1	1.691
HCL2	2.524
HCL3	3.354
HCL4	3.842
HCL5	4.175
HCL6	5.005

Calculated force:

the tension force on the hanger cable under normal traffic condition:

$L_h \approx 80.00\ m$ (longest hanger cable)

$m = (m_{HangerCable})/(g\ x\ L_h)$

$m = (3.453)/(9.81\ x\ 80.00) = 0.0044\ tons.s^2/m^2$

$f_1 = 1.691\ Hz$ (1^{st} mode frequency under normal traffic condition in Table 3.4)

from Equation 5.17:

$$1.691 = \frac{1.00}{2\ x\ 80.00}\sqrt{\frac{N_h}{0.0044}} \rightarrow N_h = 322.08\ tons$$

The calculated hanger force is 322.08 tons under normal traffic condition. For long hangers, the influences of the stiffness and the end restrains are small, but for short hangers those effects are not negligible. Ideally, all hangers should have the same force for balance. It should be kept in mind that each hanger has 370.00 tons tensile strength as it mentioned Section 2.3.4.

3.2.2. Steel Suspended Deck

Analytical expressions:

A simple, first-order linear elastic model for the deck is a beam on elastic foundation, as shown in Figure 3.11. The elastic foundation represents the flexibility of the hangers and the suspension cable.

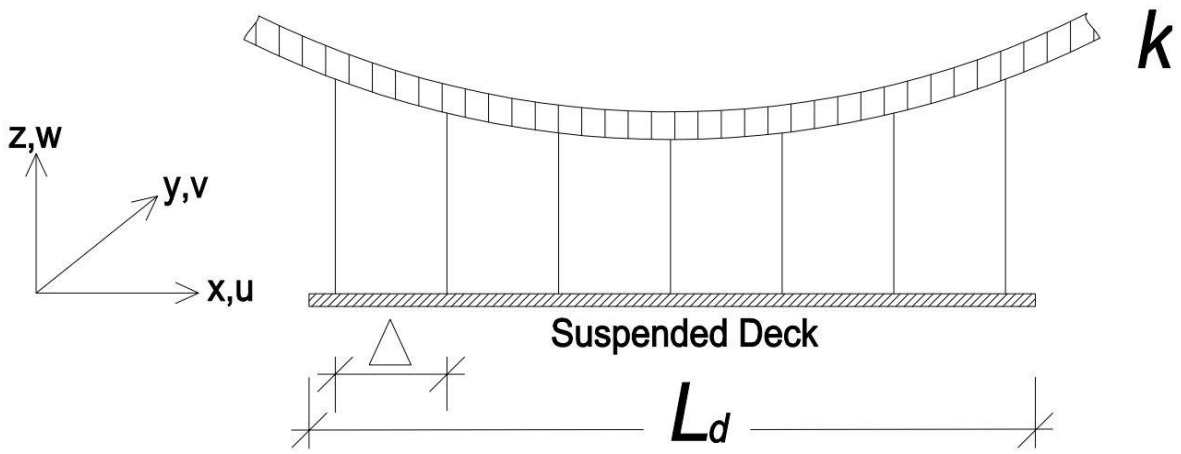

Figure 3.11. The deck modelled as a beam on elastic foundation.

Assuming that the stiffness k is approximately constant along the deck, the d^{th} natural frequency of the vertical direction is given by the following equations (Timoshenko et al., 1974 and Blevins, 1979):

$$\lambda_d = (2d+1)\frac{\pi}{2} \tag{5.18}$$

$$f_d = \frac{1}{2\pi}\sqrt{\left(\frac{\lambda_d}{L_d}\right)^4 \frac{EI}{m} + \frac{k}{\Delta m}} \tag{5.19}$$

where, E is modulus of elasticity, m mass per unit length, I is moment of inertia of the deck, Δ represents distance between the hangers, k is main cable stiffness per unit length of the deck, L_d is length of the deck in longitudinal direction and λ_d refers to the non-dimensional frequency parameter (free-free boundary conditions in vertical direction). The dimensionless frequency parameter λ_d is a function of the boundary conditions, its values for different cases can be found in Blevins (1979).

Records and frequencies identified:

Figures below point out recorded acceleration-time histories and SFAS of the steel suspended deck in vertical direction under light and heavy traffic conditions.

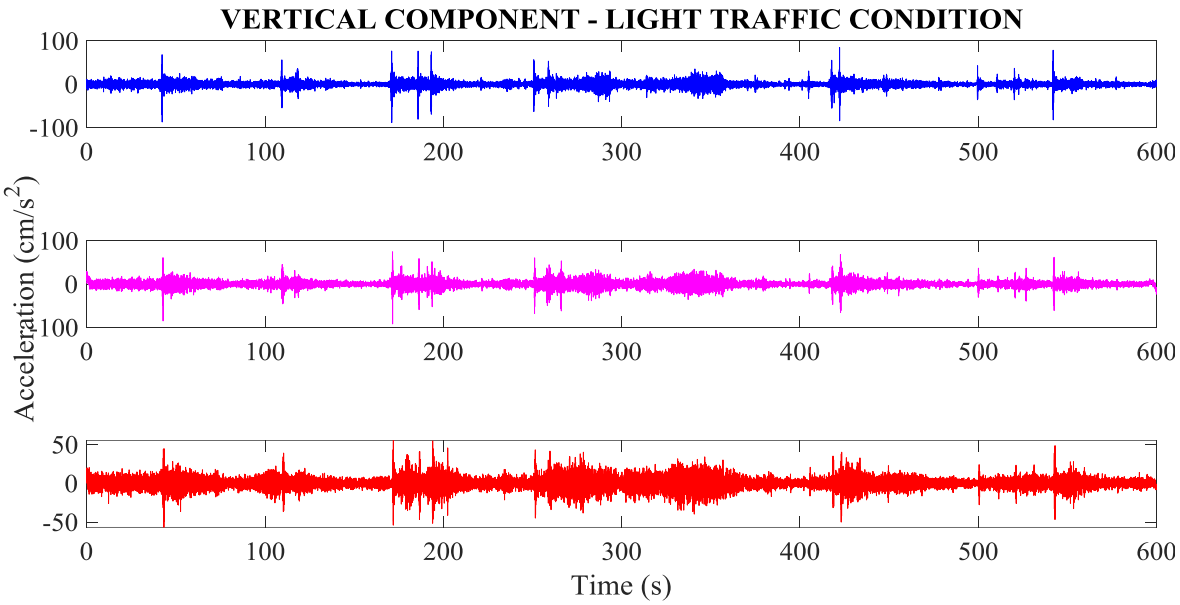

Figure 3.12. Recorded acceleration time histories for light traffic condition in vertical direction of the deck (location 1-2-3 respectively).

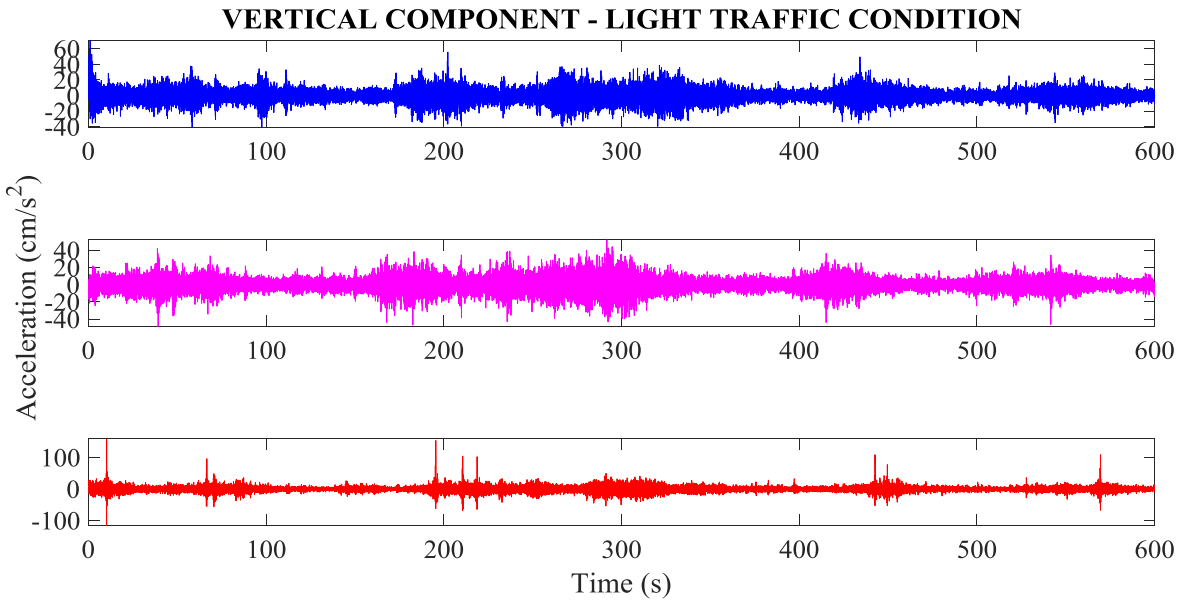

Figure 3.13. Recorded acceleration time histories for light traffic condition in vertical direction of the deck (location 4-5-6 respectively).

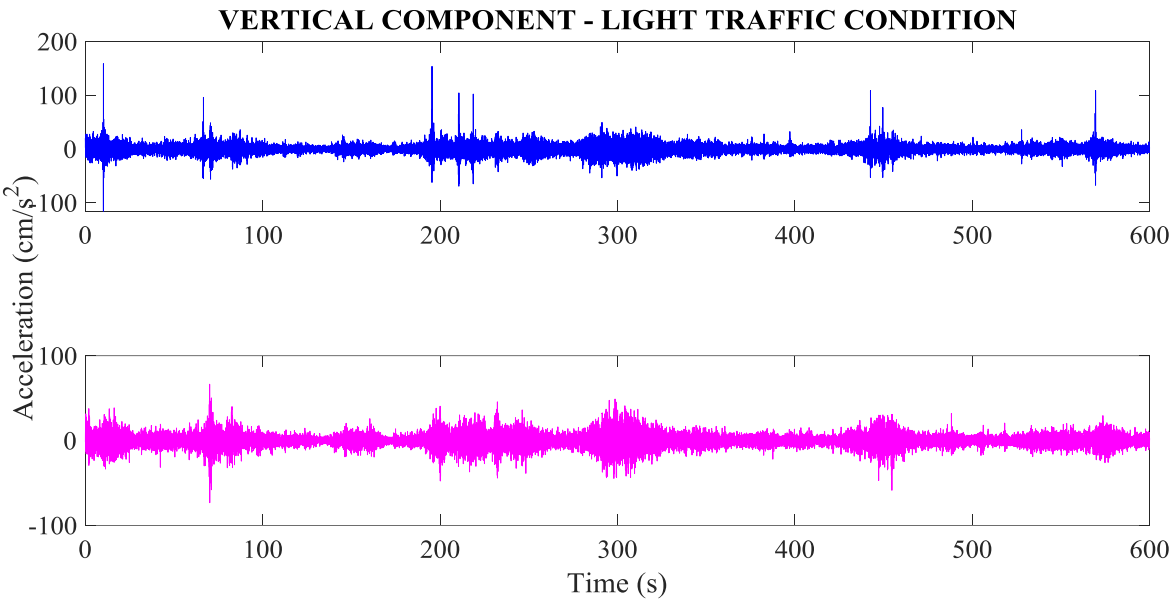

Figure 3.14. Recorded acceleration time histories for light traffic condition in vertical direction of the deck (location 7-8 respectively).

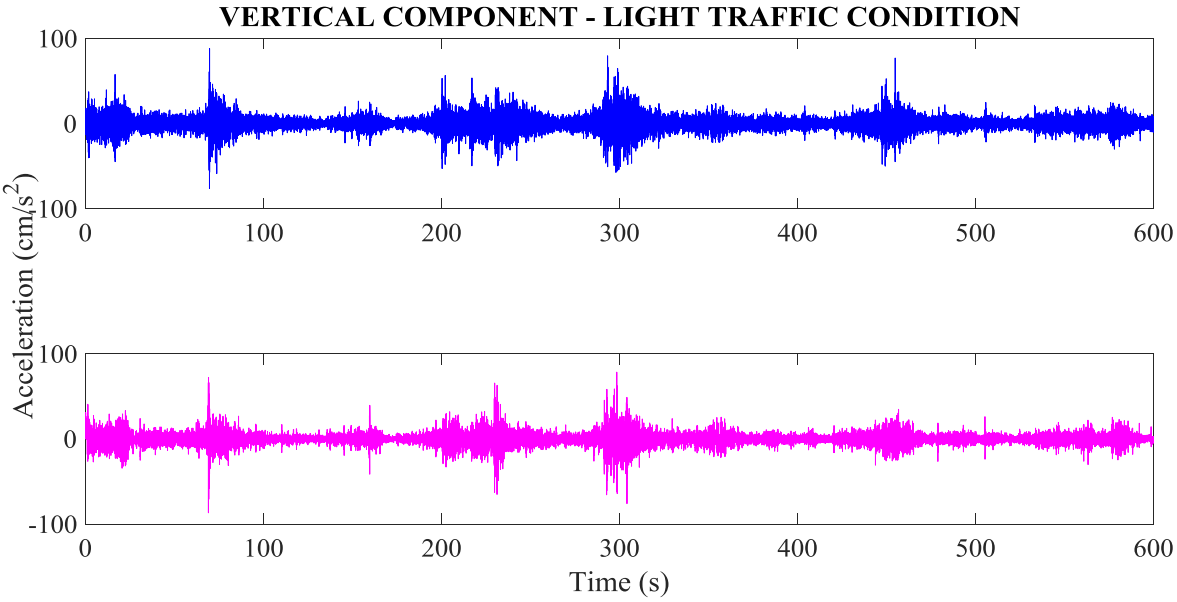

Figure 3.15. Recorded acceleration time histories for light traffic condition in vertical direction of the deck (location 9-10 respectively).

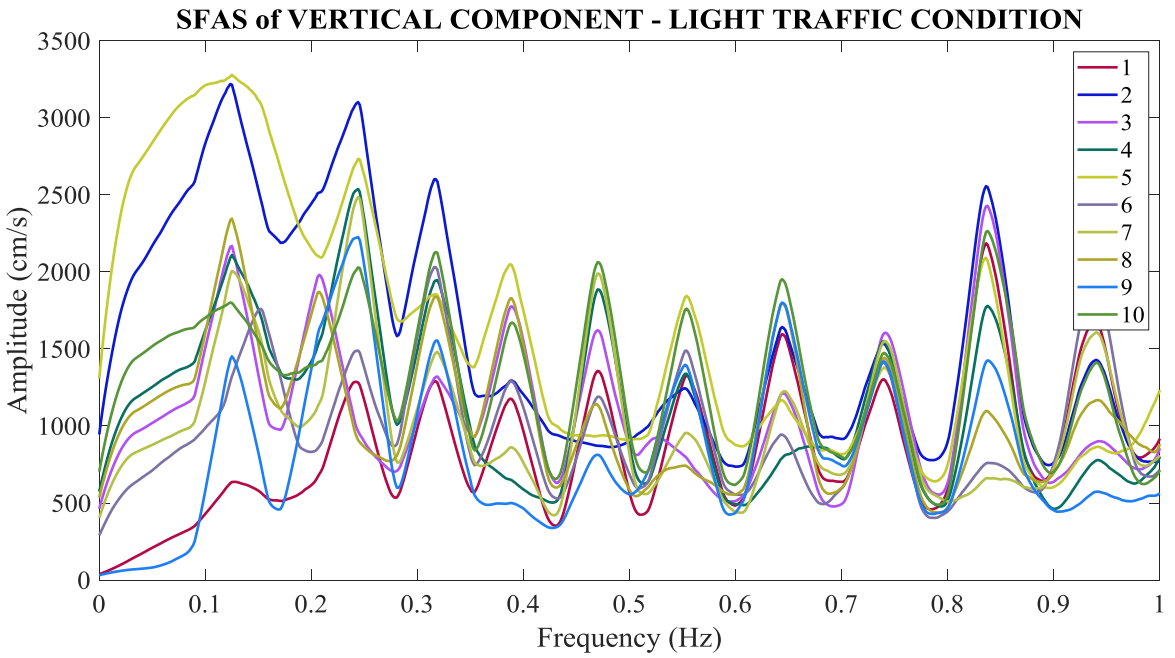

Figure 3.16. SFAS at light traffic condition in vertical direction of the deck.

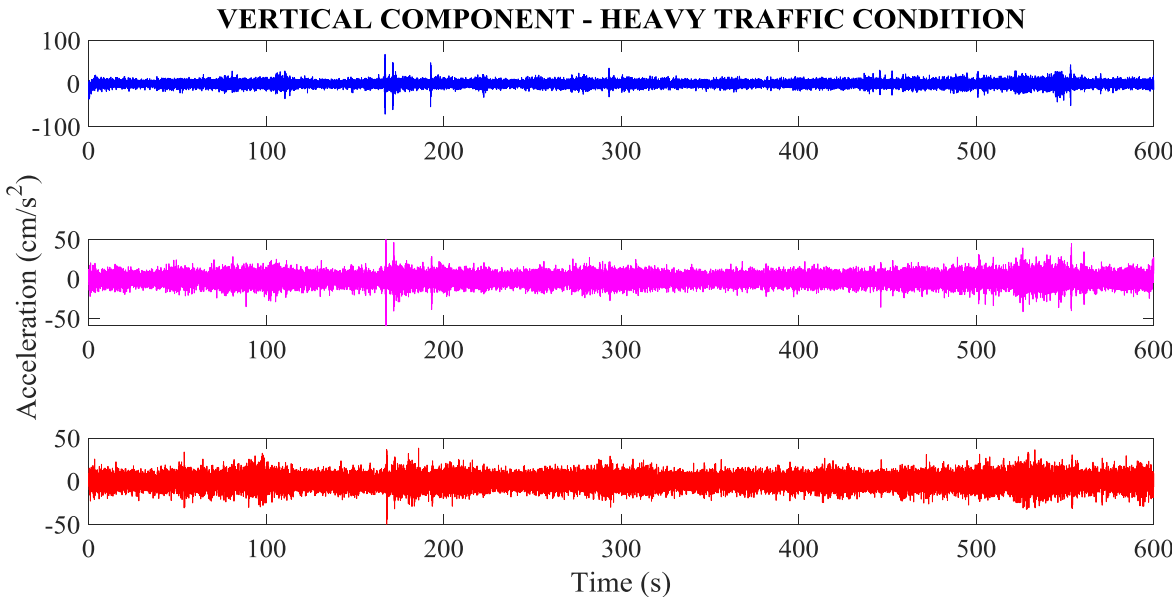

Figure 3.17. Recorded acceleration time histories for heavy traffic condition in vertical direction of the deck (location 1-2-3 respectively).

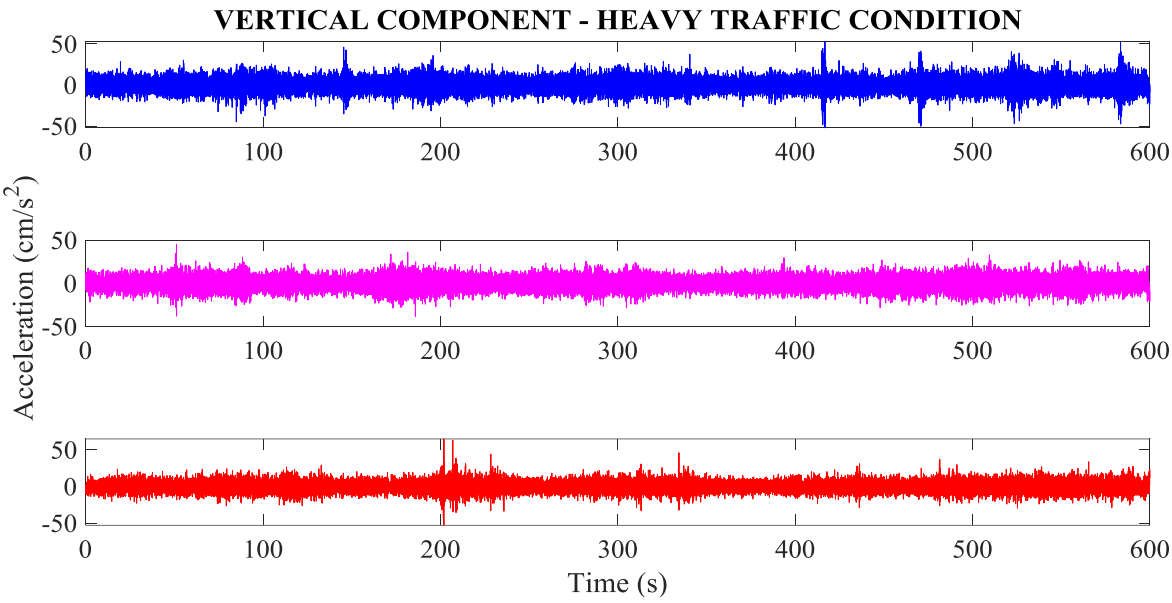

Figure 3.18. Recorded acceleration time histories for heavy traffic condition in vertical direction of the deck (location 4-5-6 respectively).

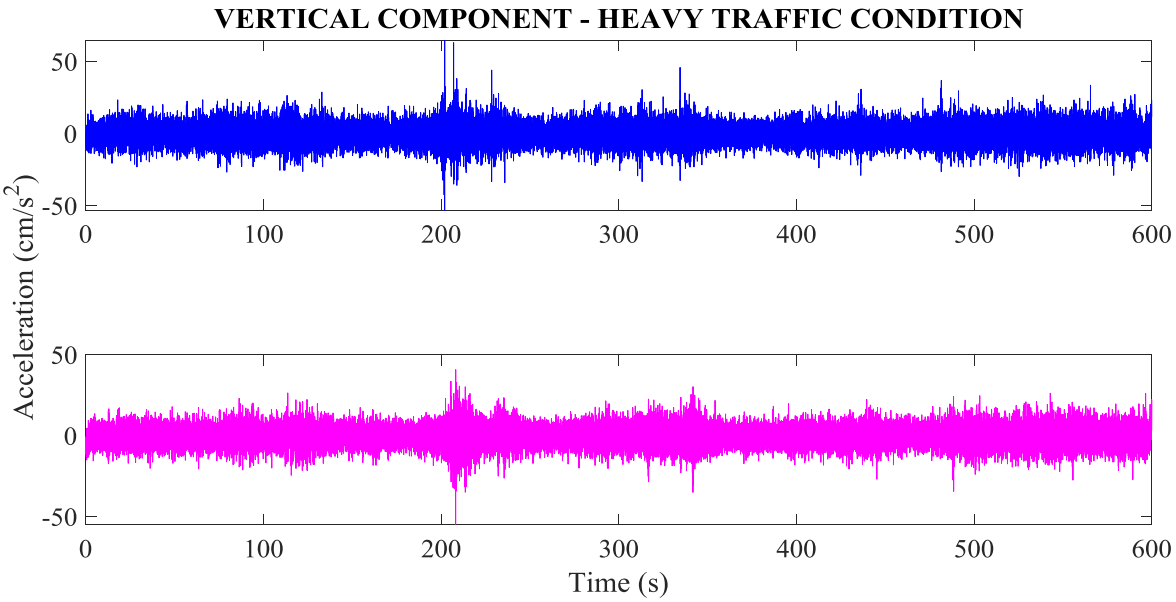

Figure 3.19. Recorded acceleration time histories for heavy traffic condition in vertical direction of the deck (location 7-8 respectively).

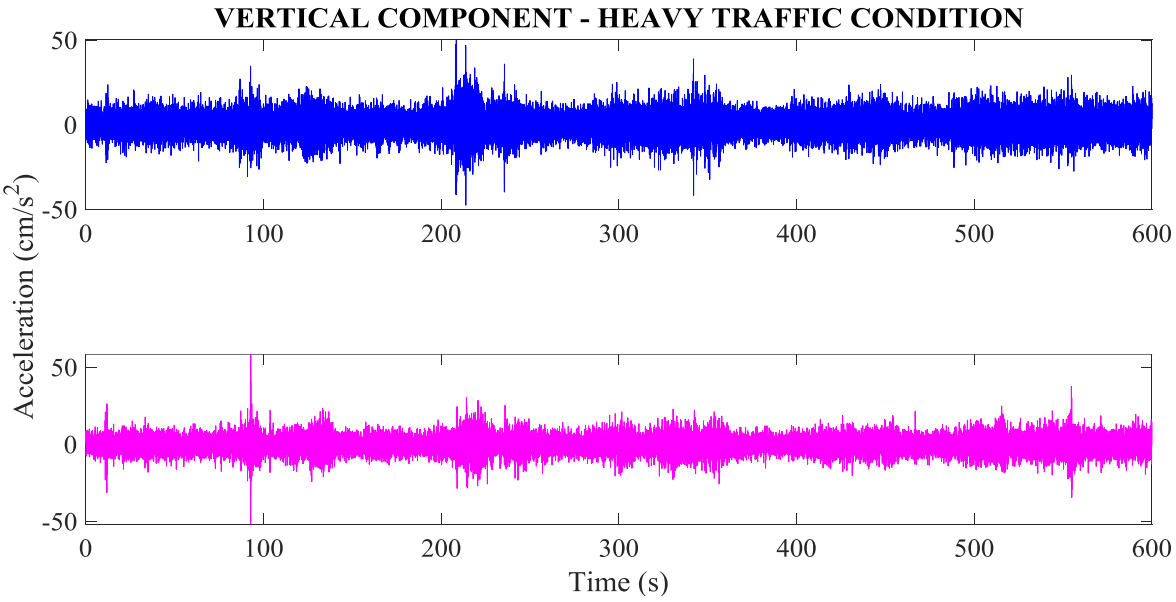

Figure 3.20. Recorded acceleration time histories for heavy traffic condition in vertical direction of the deck (location 9-10 respectively).

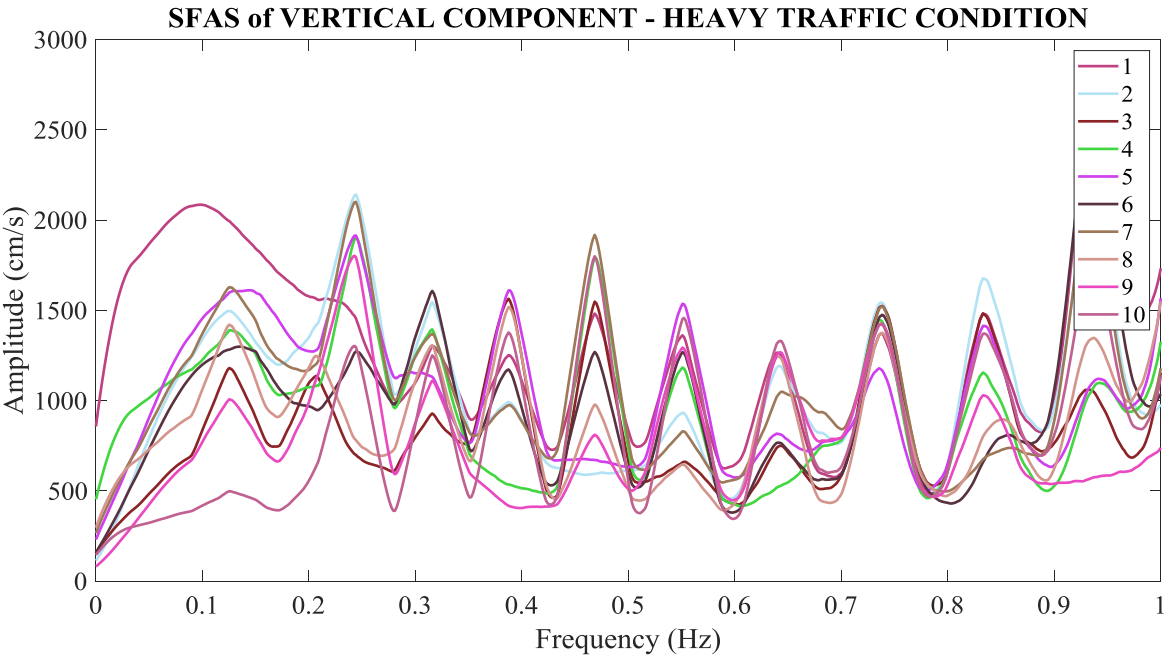

Figure 3.21. SFAS at heavy traffic condition in vertical direction of the deck.

Table 3.5 lists the frequencies of the vertical vibrations of the deck identified from Figure 3.16 and Figure 3.21. A comparison of the identified frequencies with those from the previous studies is also shown on Table 3.5. The maximum relative difference is about 5%.

Table 3.5. Comparison between experimental and previous investigations modal frequencies and their differences in vertical direction of the deck.

Modal Frequencies from Ambient Vibration Survey and 3D FE Model of the FSM Suspension Bridge									
Vertical Deck Modes		Brownjohn et al. (1992)		Apaydın et al. (2016)	Kavak (2019)		Brownjohn et al. (1992)		Apaydın et al. (2016)
		Experimental Frequency (Hz)	Theoretical Frequency (Hz)	Theoretical Frequency (Hz)	Experimental Frequency (Hz)		Error (%)		Error (%)
Number	Type and Symmetry		3D FE Model	3D FE Model	Light Traffic Condition	Heavy Traffic Condition	Experimental	3D	3D
V1	V asym	0.125	0.125	0.127	0.1251	0.1241	0.08	0.08	1.50
V2	V sym	0.155	0.159	0.155	0.1541	0.1495	0.58	3.08	0.58
V3	V sym	0.208	0.211	0.206	0.2075	0.2060	0.24	1.66	0.73
V4	V asym	0.244	0.250	0.247	0.2457	0.2426	0.70	1.72	0.53
V5	V sym	0.317	0.323	0.319	0.3174	0.3159	0.13	1.73	0.50
V6	V asym	0.389	0.396	0.390	0.3891	0.3876	0.03	1.74	0.23
V7	V sym	0.470	0.479	0.469	0.4700	0.4684	0.00	1.88	0.21
V8	V asym	0.555	0.568	0.551	0.5539	0.5508	0.20	2.48	0.53
V9	V sym	0.645	0.666	0.639	0.6439	0.6409	0.17	3.32	0.77
V10	V asym	0.741	0.772	0.730	0.7416	0.7370	0.08	3.94	1.59
V11	V sym	0.839	0.887	0.826	0.8377	0.8331	0.15	5.56	1.42
V12	V asym	0.942	-	0.924	0.9399	0.9338	0.22	-	1.72

The ambient vibration measurements of Brownjohn et al. (1992) and 3D FEM of Apaydın et al. (2016) were performed under normal traffic conditions (about 25% of the design LL). The theoretical modal frequencies were calculated assuming 2000 tons (25% of the design LL) moving load.

The flexibility of the steel suspended deck:

modulus of the elasticity, moment of inertia and length of the deck:

$E = 210000.00\,MPa = 21414040.00\,tons/m^2$ (Table 2.2)

$I = I_{yy} = 1.7318\,m^4$ (Table 2.3)

$L_d \approx L \approx 1090.36\,m$

modulus of the elasticity, cross section area and stiffness of the main span cable:

$E = 189300.00\ MPa = 19303227.00\ tons/m^2$ (Table 2.2)

$A = 0.36615\ \text{m}^2$ (Table 2.3)

$$k = 2\left(\frac{EA}{L}\right)/L_d = 2\left(\frac{19303227.00\ x\ 0.36615}{1090.36}\right)/1090.36 = 11.89\ tons/m/m$$

vertical hanger cables interval:

$\Delta = 17.92\ \text{m}$ (Section 2.3.4)

assume as $m_{LiveLoad} = 2000.00$ tons:

$$m = [(m_{Deck} + m_{LiveLoad})/(g\ x\ L_d)]$$

$$m = [(16960.00 + 2000.00)/(9.81\ x\ 1090.36)] = 1.7726\ \text{tons.s}^2/\text{m}^2$$

according to Equation 5.18, non-dimensional frequency parameter, λ_d:

$\lambda_1 = 4.71\ \lambda_2 = 7.86\ \lambda_3 = 11.0\ \lambda_4 = 14.14\ \lambda_5 = 17.28\ \lambda_6 = 20.42$

$\lambda_7 = 20.56\ \lambda_8 = 26.70\ \lambda_9 = 29.85\ \lambda_{10} = 32.99\ \lambda_{11} = 36.13\ \lambda_{12} = 39.27$

according to Equation 5.19, mode frequency in vertical direction of the deck:

$$f_d = \frac{1}{2\pi}\sqrt{\left(\frac{\lambda_d}{1090.36}\right)^4 \frac{21414040.00\ x\ 1.7318}{1.7726} + \frac{11.89}{17.92\ x\ 1.7726}}$$

$f_1 = 0.111\ f_2 = 0.135\ f_3 = 0.171\ f_4 = 0.22\ f_5 = 0.28\ f_6 = 0.353$

$f_7 = 0.437\ f_8 = 0.534\ f_9 = 0.643\ f_{10} = 0.764\ f_{11} = 0.897\ f_{12} = 1.042$

Table 3.6 and Table 3.7 show the measured and calculated modal frequencies and their comparison with previous studies. The maximum relative difference is about 19%.

Table 3.6. Comparison between theoretical and previous investigations modal frequencies and their differences in vertical direction of the deck.

Modal Frequencies from Ambient Vibration Survey and 3D FE Model of the FSM Suspension Bridge								
Vertical Deck Modes		Brownjohn et al. (1992)		Apaydın et al. (2016)	Kavak (2019)	Brownjohn et al. (1992) Error (%)		Apaydın et al. (2016) Error (%)
Number	Type and Symmetry	Experimental Frequency (Hz)	Theoretical Frequency (Hz) 3D FE Model	Theoretical Frequency (Hz) 3D FE Model	Theoretical Frequency (Hz)	Experimental	3D	3D
V1	V asym	0.125	0.125	0.127	0.1110	11.22	11.22	12.62
V2	V sym	0.155	0.159	0.155	0.1351	12.81	15.00	12.81
V3	V sym	0.208	0.211	0.206	0.1714	17.59	18.77	16.79
V4	V asym	0.244	0.250	0.247	0.2198	9.94	12.10	11.03
V5	V sym	0.317	0.323	0.319	0.2802	11.61	13.26	12.17
V6	V asym	0.389	0.396	0.390	0.3527	9.33	10.93	9.56
V7	V sym	0.470	0.479	0.469	0.4373	6.95	8.70	6.76
V8	V asym	0.555	0.568	0.551	0.5340	3.78	5.98	3.08
V9	V sym	0.645	0.666	0.639	0.6428	0.34	3.49	0.59
V10	V asym	0.741	0.772	0.730	0.7637	3.06	1.08	4.61
V11	V sym	0.839	0.887	0.826	0.8966	6.87	1.08	8.55
V12	V asym	0.942	-	0.924	1.0416	10.58	-	12.73

Table 3.7. Comparison between theoretical and experimental modal frequencies and their differences in vertical direction of the deck.

Modal Frequencies from Ambient Vibration Survey and Analytical Formulas for the FSM Suspension Bridge					
Vertical Deck Modes	Kavak (2019)				
	Experimental Frequency (Hz)		Theoretical Frequency (Hz)	Error (%)	
Number	Light Traffic Condition	Heavy Traffic Condition	Normal Traffic Condition		
V1	0.1251	0.1241	0.1110	11.29	10.58
V2	0.1541	0.1495	0.1351	12.30	9.60
V3	0.2075	0.2060	0.1714	17.40	16.79
V4	0.2457	0.2426	0.2198	10.56	9.42
V5	0.3174	0.3159	0.2802	11.72	11.31
V6	0.3891	0.3876	0.3527	9.35	9.00
V7	0.4700	0.4684	0.4373	6.95	6.64
V8	0.5539	0.5508	0.5340	3.59	3.05
V9	0.6439	0.6409	0.6428	0.17	0.29
V10	0.7416	0.7370	0.7637	2.97	3.62
V11	0.8377	0.8331	0.8966	7.03	7.62
V12	0.9399	0.9338	1.0416	10.83	11.55

Relative difference between in this study and previous studies are high in the vertical direction of the deck in some cases. Interestingly, in higher modes, relative differences decrease.

3.2.3. Steel Towers

Analytical expressions:

Towers of a suspension bridge are basically cantilever beams subjected to large axial compression forces. The t^{th} natural frequency of such a cantilever is given by the following equations (Blevins, 1979):

$$f_t = \frac{\lambda_t^2}{2\pi h^2}\sqrt{\frac{EI}{m}}\left(1 + \frac{P\lambda_1^2}{P_b\lambda_t^2}\right) \tag{5.20}$$

where, h is *h*eight, h_b is buckling length, EI is flexural rigidity, m is mass per unit length, P_b is buckling load and P is axial compression load on the tower. λ_t defines to the non-dimensional frequency parameter and it is a function of the clamped-free boundary conditions in lateral direction, its values for different cases can be found in Blevins (1979). The buckling load of the tower is given by:

$$P_b = \frac{\pi^2 EI}{4h_b^2} \tag{5.21}$$

Table 3.8. Non-dimensional frequency parameter for clamped-free multispan beam with pinned intermediate supports (Blevins, 1979).

Number of Spans	**Mode Number**					
	1	2	3	4	5	6
1	1.875	4.694	7.855	11.000	14.140	17.280
2	1.570	3.923	4.707	7.058	7.842	10.190
3	1.541	3.570	4.283	4.720	6.707	7.430
4	1.539	3.403	3.928	4.450	4.723	6.545
5	1.539	3.316	3.706	4.148	4.538	4.724
6	1.539	3.265	3.563	3.927	4.292	4.592
7	1.539	3.233	3.466	3.767	4.086	4.389
8	1.539	3.213	3.399	3.649	3.926	4.204
9	1.539	3.198	3.349	3.560	3.802	4.051
10	1.539	3.187	3.312	3.492	3.703	3.927

Records and frequencies identified:

Figures below demonstrate recorded acceleration-time histories and SFAS of towers in lateral direction.

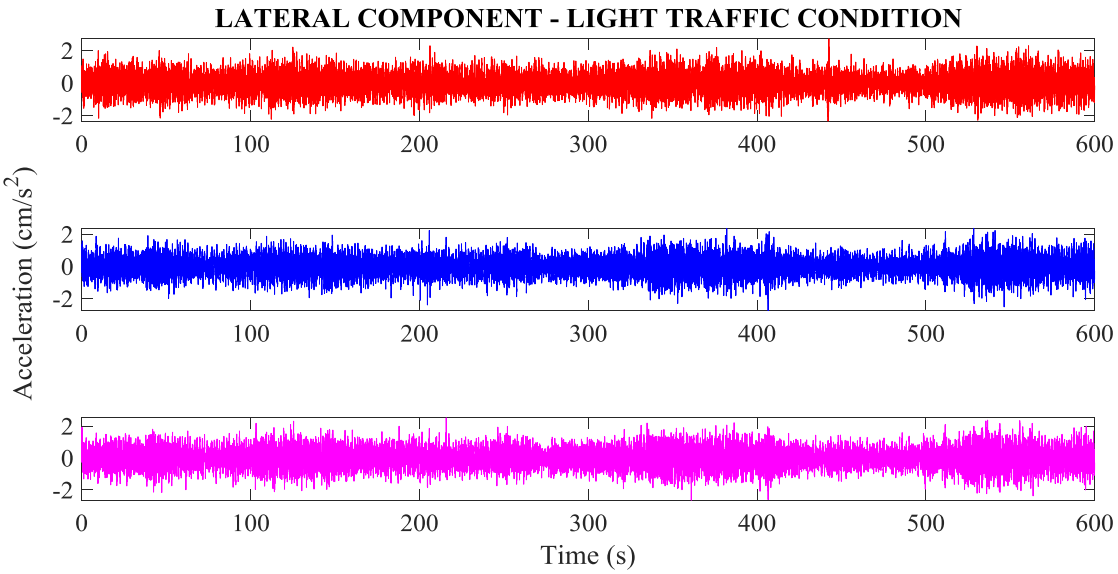

Figure 3.22. Recorded acceleration-time histories for light traffic condition in lateral direction of the towers (location 13-15-16 respectively).

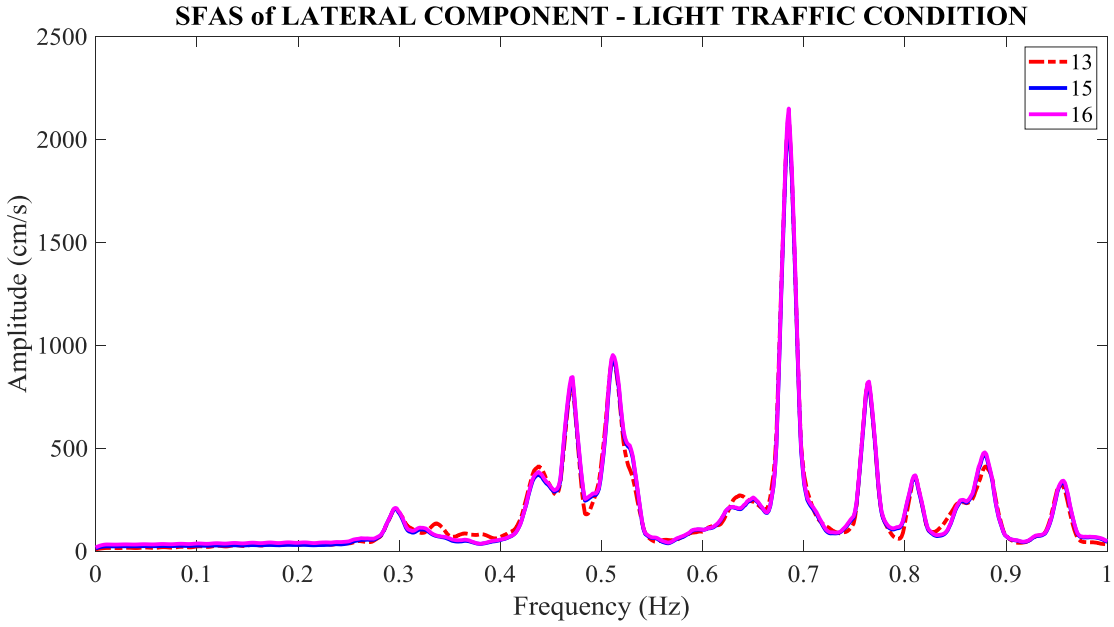

Figure 3.23. SFAS at light traffic condition in lateral direction of the towers.

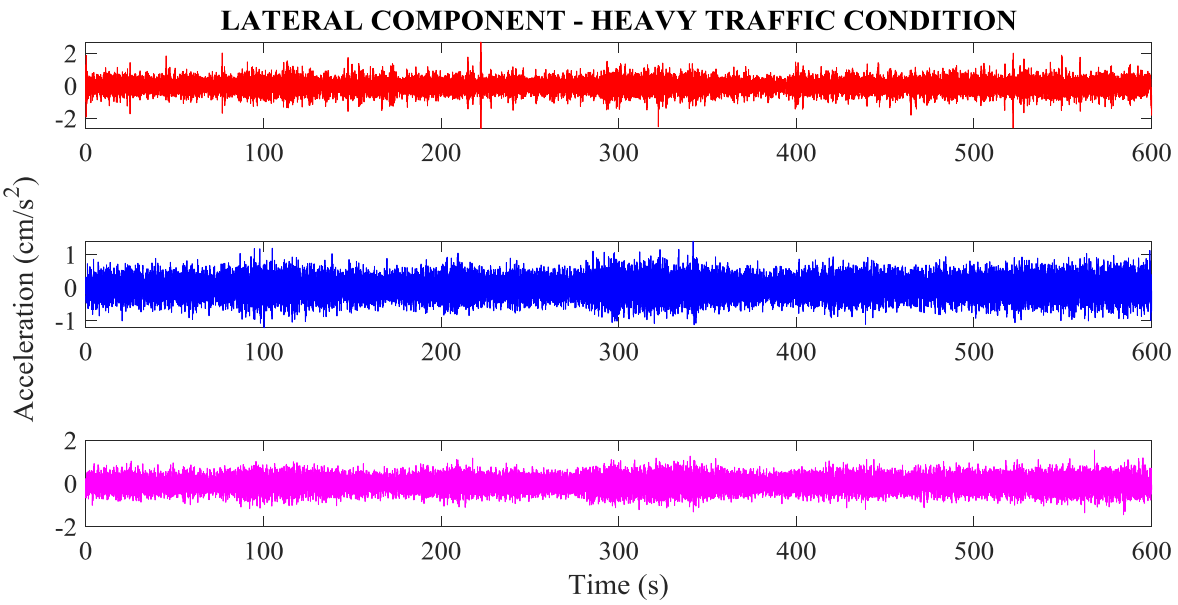

Figure 3.24. Recorded acceleration-time histories for heavy traffic condition in lateral direction of the towers (location 13-15-16 respectively).

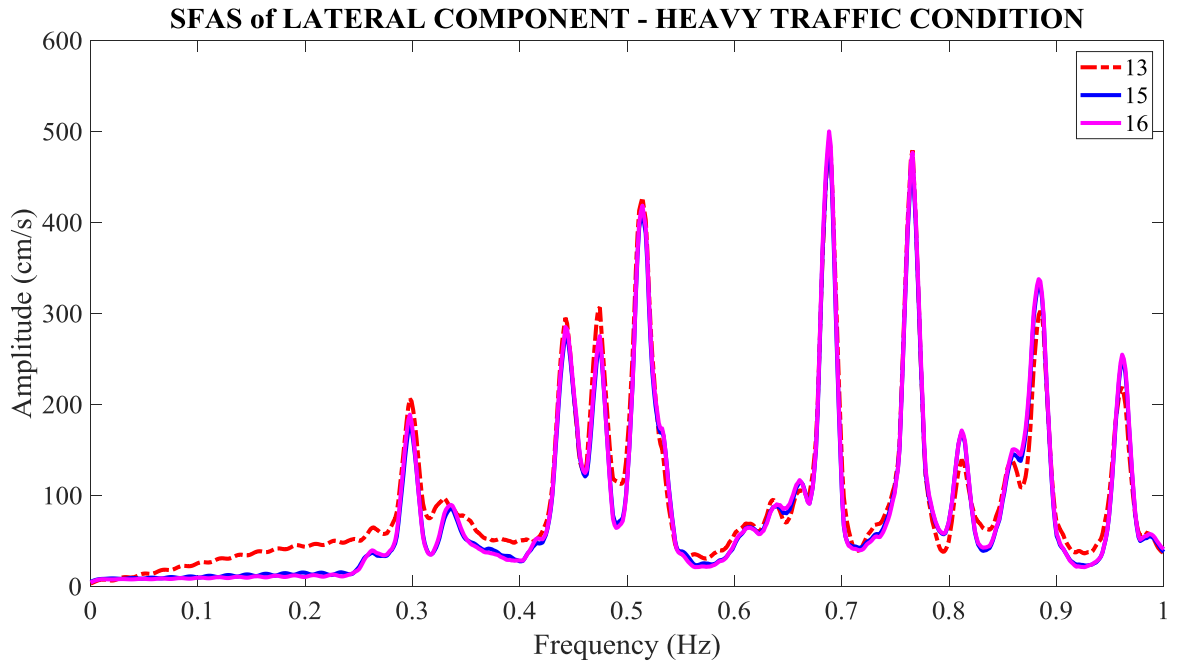

Figure 3.25. SFAS at heavy traffic condition in lateral direction of the towers.

Table 3.9 lists the natural frequencies of the towers in lateral direction, identified from Figure 3.23 and Figure 3.25 in light and heavy traffic conditions.

Table 3.9. Comparison between experimental and previous investigations modal frequencies and their differences in lateral direction of the towers.

Modal Frequencies from Ambient Vibration Survey and 3D FE Model of the FSM Suspension Bridge									
Lateral Tower Modes		Brownjohn et al. (1992)		Apaydın et al. (2016)	Kavak (2019)		Brownjohn et al. (1992)		Apaydın et al. (2016)
		Experimental Frequency (Hz)	Theoretical Frequency (Hz)	Theoretical Frequency (Hz)	Experimental Frequency (Hz)		Error (%)		Error (%)
Number	Participation		3D FE Model	3D FE Model	Light Traffic Condition	Heavy Traffic Condition	Experimental	3D	3D
TL1	Tower+Deck	0.287	0.288	0.286	0.299	0.296	3.14	2.78	3.50
TL2	Tower+Deck	0.295	0.303	0.295	0.337	0.336	13.80	10.79	13.80
TL3	Tower+Deck	0.432	0.421	0.468	0.443	0.443	2.43	5.11	5.45
TL4	Tower+Deck	0.464	0.476	0.476	0.473	0.472	1.62	0.95	0.95
TL5	Tower+Deck	0.503	0.543	0.509	0.514	0.511	1.63	5.86	0.43
TL6	Tower	0.520	0.605	0.517	-	-	-	-	-
TL7	Tower	0.630	0.649	0.601	-	-	-	-	-
TL8	Tower	0.673	0.661	0.678	-	-	-	-	-
TL9	Tower	0.691	0.716	0.686	0.688	0.685	0.85	4.32	0.13
TL10	Tower	0.753	0.768	0.767	0.766	0.765	1.53	0.46	0.33
TL11	Tower	0.802	0.846	0.825	0.812	0.810	1.02	4.23	1.79
TL12	Tower+Deck	0.866	0.934	0.881	0.884	0.879	1.49	5.90	0.24
TL13	Tower	0.937	0.950	0.955	0.961	0.957	2.10	0.71	0.18

Except the 2nd (13.80%) mode, there is close agreement between the experimental and theoretical modal frequencies of the tower in lateral direction. The relative difference for the 1st mode is 3.50%. Lateral tower mode *L6*, *L7* and *L8* found by Brownjohn et al. (1992) and Apaydın et al. (2016) but in this ambient vibration survey, it was not found such modes.

Calculated forces:

axial load on the tower under DL condition:

$f_1 = 0.299$ (*1st* mode frequency under light traffic condition in Table 3.9)

assume as $m_{LiveLoad} = 0.00$ tons:

$$m = [(m_{Tower})/(g\ x\ h)]/2 + [m_{LiveLoad}/(g\ x\ L)]/2$$

$$m = [(6820)/(9.81\ x\ 106.10)]/2 + [0.00/(9.81\ x\ 1090.36)]/2$$

$$m = 3.2762\ \text{tons.}\,\text{s}^2/\text{m}^2$$

$\lambda_1 = 1.875$ (*1st* mode number with one span in Table 3.8)

$E = 210000.00\ MPa = 21414040.00\ tons/m^2$ (Table 2.2)

$I_{zz} = I_{Avarage} \approx 3.16621\ m^4$ (Table 2.3)

$h_b \approx 57.85\ m$

$h = 106.10\ m$

from Equation 5.21:

$$P_b = \frac{\pi^2\ x\ 21414040.00\ x\ 3.16621}{4\ x\ 57.85^2} \rightarrow P_b = 49988.65\ tons$$

from Equation 5.20:

$$0.299 = \frac{1.875^2}{2\ x\ \pi\ x\ 106.10^2}\sqrt{\frac{21414040.00\ x\ 3.16621}{3.2762}}\left(1 + \frac{P\ x\ 1.875}{49988.65\ x\ 1.875}\right)$$

$P = 16113.67\ tons$

axial load on the tower under DL+LL condition:

$f_1 = 0.296$ (*1st* mode frequency under heavy traffic condition in Table 3.9)

assume as $m_{LiveLoad} = 8000.00$ tons:

$$m = [(m_{Tower})/(g\ x\ h)]/2 + [m_{LiveLoad}/(g\ x\ L)]/2$$

$$m = [(6820)/(9.81\ x\ 106.10)]/2 + [8000.00/(9.81\ x\ 1090.36)]/2$$

$$m = 3.6502 \text{ tons.s}^2/\text{m}^2$$

from Equation 5.20:

$$0.296 = \frac{1.875^2}{2\ x\ \pi\ x\ 106.10^2}\sqrt{\frac{21414040.00\ x\ 3.16621}{3.6502}}\left(1 + \frac{P\ x\ 1.875}{49988.65\ x\ 1.875}\right)$$

$$P = 19084.68\ tons$$

It is seen from this study that the calculated tower axial force under DL is 158.02 MN (16113.67 tons) and there is 12.85% and 4.44% difference with analytical study and the record book of the bridge, respectively. The axial force under DL+LL is 187.16 MN (19084.68) and relative difference is much higher than under DL. There is 15.65% and 6.04% difference with analytical study and the record book of the bridge, respectively.

3.3. Summary of Comparisons with Previous Studies

This study presents an alternative method for system identification of suspension bridges from their vibration records. Based on some simplifying assumptions, this study first develops the equations that relate the element forces to the fundamental frequency of that element.

Table 3.10 summarizes the comparisons of the calculated member forces in this study with those from the finite element study by Apaydın (2002) and the record book of the bridge (1989). The results are found to be consistent.

Table 3.10. Forces on structural components of FSM suspension bridge.

	Hanger Cable (tons)	Forces on Tower Top (Selected Location)					
		Back-stay Cable		Main Span Cable		Tower	
		DL (MN)	DL + LL (MN)	DL (MN)	DL + LL (MN)	DL (MN)	DL + LL (MN)
Results From The Ambient Vibration Survey (Kavak, 2019)	322.08 (Normal Traffic)	243.00 (Normal Traffic)		163.63	219.29	158.02	187.16
Results From The Analytical Model (Apaydin, 2002)	-	173.66	239.32	165.05	229.25	140.02	161.84
Results From The Original Calculation Report of The Brdige (IHI, MHI, NKK Corp.)	-	200.20	248.10	187.00	232.50	151.30	176.50

4. SUMMARY AND CONCLUSION

This dissertation presents analytical expressions that relate the dominant frequencies of the main components of a suspension bridge to the forces on them. The equations are based on the assumption of first-order approximation and linear behaviour. These expressions can be used to calculate forces in the main components of the bridge (i.e., main suspension cables, back-stay cables, hangers and towers) and the flexibility of the steel suspended deck by identifying their dominant frequencies through measurements under different traffic conditions.

Accelerations of ambient vibrations were measured on the deck, towers, back-stay cables, main span cables and hangers of the FSM Bridge. The data were processed by de-trending and filtering. Dominant frequencies of the main components are identified from the FAS under different traffic loads.

The results obtained under heavy and light traffic conditions do not differ much. It may be concluded that variations on traffic loads have negligible effect to the response of long-span suspension bridges. The results also show that, when compared to those of the previous experimental and analytical studies, the frequencies and the loads obtained from this study are in good agreement with the previous studies.

REFERENCES

Abdel-Ghaffar, A.M., "Dynamic Analysis of Suspension Bridge Structures", *EERL Report 76-01,* California Institute of Technology, Pasadena, California, 1976.

Abdel-Ghaffar, A.M.; Stringfellow, R.G., "Response of Suspension Bridges to Travelling Earthquake Excitations, Part II. Lateral Response", *Soil Dyn. Earthq. Eng. 3*, 73–81, 1984.

Andersson A.: "Evaluating Cable Forces in Cable Supported Bridges Using Methods of Structural Vibrations", *Royal Institute of Technology Department of Civil and Architectural Engineering*, Stockholm, Sweden, 2007.

Andersson, A., Sundquist, H., Karoumi, R., "Evaluating Cable Forces in Cable Supported Bridges Using the Ambient Vibration Method", *The International Conference on Bridge Engineering - Challenges in the 21st Century*, November 1-3, 2006, Hong Kong, 2006.

Apaydın, N.M., "Seismic Analysis of Fatih Sultan Mehmet Suspension Bridge", *Ph.D. Thesis, Department of Earthquake Engneering, Bogazici University,* Istanbul, Turkey, 2002.

Apaydın, N.M., "Earthquake Performance Assessment and Retrofit Investigations of Two Suspension Bridges in Istanbul", *Soil Dyn. Earthq. Eng. 30*, 702–10, 2010.

Apaydın, N.M., Kaya, Y., "Free Vibration Differences Between Traffic and No Traffic Condition On Suspension Bridge", *The 14th World Conference on Earthquake Engineering (14WCEE)*, 12-17 October 2008, Beijing, China.

Apaydın, N.M.; Kilic, S.A,; Raatschen, H.J.; Körfgen, B,; Astaneh-Asl, A., "Finite Element Model of the Fatih Sultan Mehmet Suspension Bridge Using Thin Shell Finite Elements", *Arab J Sci Eng*, September 20, 2016.

Blevins, R.D., "Formulas for Natural Frequency and Mode Shape", *Von Nostrand Reinhold Co.,* New York, 1979.

Brownjohn, J.M.W., Severn, R.T., Dumanoglu, A.A., "Ambient Vibration Survey of The Fatih Sultan Mehmet (Second Bosporus) Suspension Bridge", *Earthq. Eng. Struct. D. 21,* 907–24, 1992.

Brownjohn, J.M.W., Dumanoglu, A.A., Severn, R.T., "Full-Scale Dynamic Testing of The 2nd Bosporus Suspension Bridge", *In, Proceedings of the 10th World Conference on Earthquake Engineering,* Madrid, Spain, pp. 2695–700, 1992.

Chopra AK., "Dynamics of structures: Theory and Applications to Earthquake Engineering, 2nd edition" *Upper Saddle Prentice Hall,* New Jersey, 2001.

Dumanoglu, A.A.; Brownjohn, J.M.W.; Severn, R.T., "Seismic Analysis of The Fatih Sultan Mehmet (2nd Bosporus) Suspension Bridge", *Earthq. Eng. Struct. D. 21,* 881–906, 1992.

E. Caetano., "On the Identification of Cable Force from Vibration Measurements", *IABSE-IASS Symposium,* London, 2011.

Gerardin, M., and Rixen, D., "Mechanical Vibrations", *John Wiley & Sons,* New York, 1997.

IHI., MHI., NKK Corp., "Record Book for the Fatih Sultan Mehmet Suspension Bridge and its Appendix", Tokyo, 1989.

Irvine, H.M., "Cable Structures", *The MIT Press Series in Structural Mechanics,* 1981.

Irvine, H.M., Griffin, J.H., "Int. J. Earthqu. Eng. Struct. Dyn", *4:389-402,* 1976.

J.L, Luco., J. Turmo., "Effect of Hanger Exibility on Dynamic Response of Suspension Bridges", *J. Engineering Mechanics 136,* 1444-1459, 2010.

Kaya, Y., "Tools and Techniques for Real Time Modal Identification", *PhD Dissertation, Earthquake engineering Department, Boğaziçi University,* Istanbul, Turkey, 2009.

Kaya, Y., and Şafak, E., "Structural Health Monitoring & Damage Detection", *Proceedings of the 31st IMAC, A Conference and Exposition on Structural Dynamics,* Vol.4, pp.569, 2013.

Mars, P., and Hardy, D., "Mesure des Efforts dans les Structures a Cables", *Annales TP Belgique,* No. 6, pp. 515-531, 1985.

Mathworks., "MATLAB-The Language of Technical Computing", *The Math Works, Natick,* USA, 2013.

Soyöz, S., Feng, M.Q., Shinozuka, M., "Structural Reliability Estimation with Vibration-based Identified Parameters", *Journal of Engineering Mechanics,* ASCE, Vol.136, No.1, pp. 100-106, 2010.

Şafak, E., "Analysis of Ambient Ground and Structural Vibration Data", *Annual meeting of the seismological society of America,* Incline Village/Lake Tahoe, 2005.

Şafak, E., "Analysis of Real Time Data from Instrumented Structures", *The 13th World Conference on Earthquake Engineering,* Paper No.2193, Vancouver, B.C., Canada, August 1–6, 2004.

Şafak, E., "Identification of Linear Structures Using Discrete-Time Filters", *Journal of Structural Engineering,* Vol. 117, No. 10, pp. 3064-3085, 1991.

Şafak, E., "Models and Methods to Characterize Site Amplification from a Pair of Records", *Earthquake Spectra,* Vol.13, No.1, pp97-129, 1997.

Şafak, E., "Monitoring and System Identification of Suspension Bridges: An Alternative Approach", *Istanbul Bridge Conference,* Istanbul, Turkey, 8-10 August 2016.

Şafak, E., Çaktı, E., "Simple Techniques to Analyze Vibration Records From Buildings", *Proceedings of the 7th European Workshop on Structural Health Monitoring,* 8-11 July 2014, Nantes, France, 2014.

Şafak, E., Çaktı, E., and Kaya, Y., "Recent Developments on Structural Health Monitoring and Data Analyses", *Earthquake Engineering in Europe, Geotechnical, Geological, and Earthquake Engineering,* Chapter 14, Vol. 17, pp. 331-355, 2010.

Timoshenko, S.P., and Young, D.H., "Theory of Structures", *McGraw-Hill Book Co.,* New York, 1965.

Timoshenko, S.P., Young, D.H., and Weaver, JR,W., "Vibration Problems in Engineering", *John Wiley & Sons*, New York, 1974.

Zhang, J.; Prader, J.; Moon, F.; Aktan, E.; Wu, Z.S., "Challenges and Strategies in Structural Identification of a Long Span Suspension Bridge", *In, 6th International Workshop on Advanced Smart Materials and Smart Structures Technology (ANCRiSST),* Dalian, pp 1–12, 2011.

Zhi, Fang., and Jian-qun, Wang., "Practical Formula for Cable Tension Estimation by Vibration Method", *American Society of Civil Engineers,* 10.1061/(ASCE)BE, 1943-5592.0000200, January 1st, 2012.